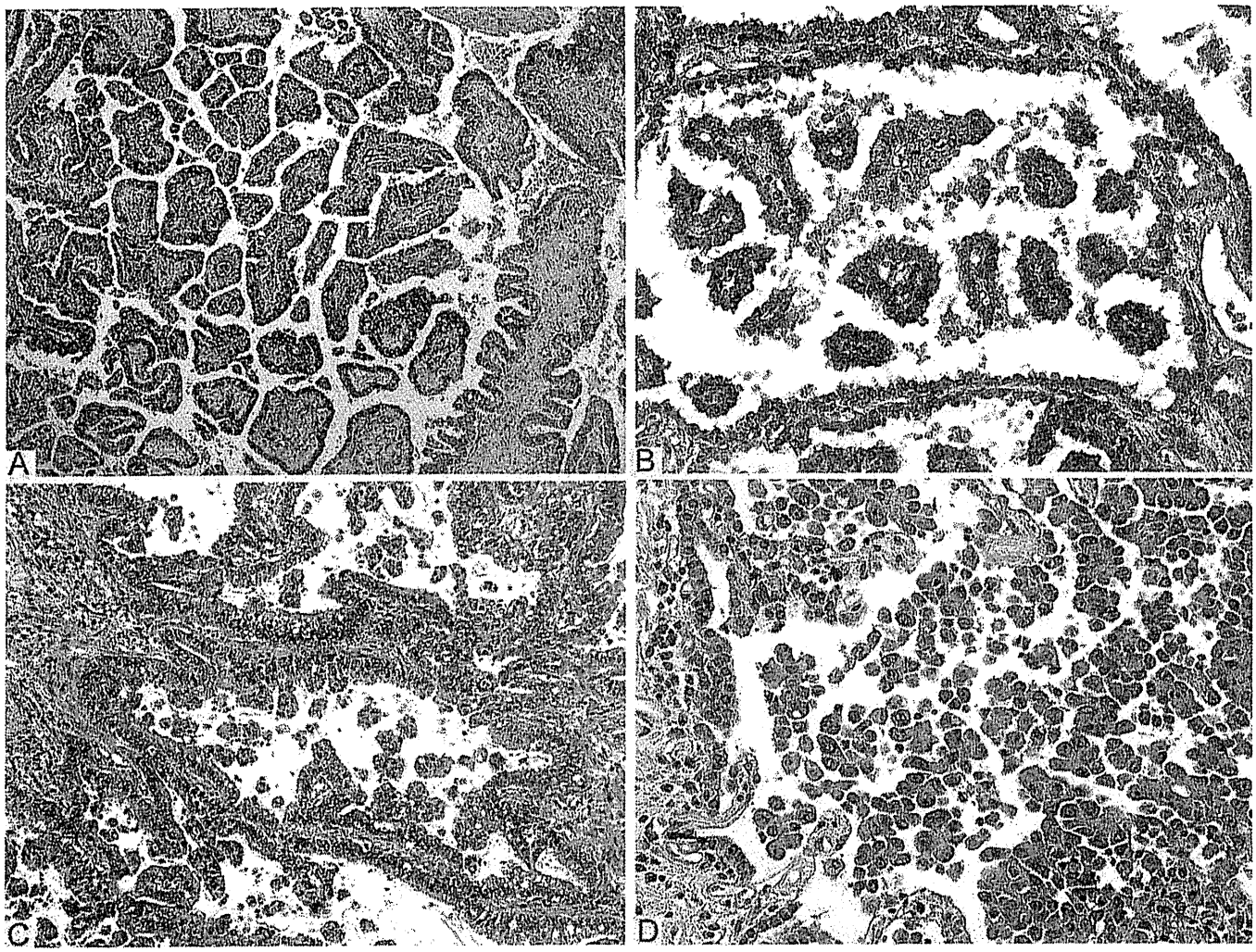

Figure 7. *Papillary and micropapillary adenocarcinoma. A, Papillary adenocarcinoma consists of malignant cuboidal to columnar tumor cells growing on the surface of fibrovascular cores. B, Papillary adenocarcinoma consisting of intra-alveolar papillary structures with fibrovascular cores. Although there is a cuboidal lining of tumor cells around the airspace in a lepidic fashion, this pattern should be classified as papillary adenocarcinoma. C, Micropapillary adenocarcinoma. Within the airspaces the tumor is growing in papillary structures lacking fibrovascular cores. Although there are some true papillary areas with fibrovascular cores, and some tumor cells growing in a lepidic pattern along the surfaces of the airspaces, most of this pattern should be regarded as micropapillary. D, Micropapillary adenocarcinoma. This tumor is spreading through the alveolar space with a spectrum of small papillary structures lacking fibrovascular cores to single dyscohesive cells (hematoxylin-eosin, original magnifications ×4 [A], ×20 [B and C], and ×40 [D]).*

clinical, radiologic, pathologic, and genetic differences from the tumors formerly classified as nonmucinous BAC (Table 6). In particular, these tumors show a very strong correlation with *KRAS* mutation and lack of *EGFR* mutation, while nonmucinous adenocarcinomas are more likely to show *EGFR* mutation and only occasionally *KRAS* mutation (Table 6). Therefore, in the new classification, these tumors are now separated into different categories (Table 1). The neoplasms formerly termed *mucinous bronchioloalveolar carcinoma* (*mucinous BAC*), are now recognized as having invasive components in most cases, and are classified as "invasive mucinous adenocarcinoma (formerly mucinous BAC)," or mucinous AIS or MIA if they meet the criteria outlined in Tables 2 and 3.

Rationale for Including Mucinous Cystadenocarcinoma in Colloid Adenocarcinoma.—Tumors formerly classified as "mucinous cystadenocarcinoma" are very rare and they probably represent part of the spectrum of colloid adenocarcinoma. Therefore, we suggest that these adenocarcinomas, which consist of unilocular or oligolocular cystic structures by imaging and/or gross examination, be included in the category of colloid adenocarcinoma.[110] For such tumors, a comment could be made that the tumor resembles that formerly classified as mucinous cystadenocarcinoma.

Rationale for Removing Clear Cell and Signet Ring Carcinoma as Adenocarcinoma Subtypes.—Clear cell and signet ring cell features are now regarded as cytologic changes that may occur in association with multiple histologic patterns.[111,112] Thus, their presence and extent should be recorded, but data are not available that show a clinical significance beyond a strong association with the solid subtype. They are not considered to be specific histologic subtypes, although associations with molecular features are possible, such as the recent observation of a solid pattern with greater than 10% signet ring cell features in up to 56% of tumors from patients with echinoderm microtubule-associated protein-like 4 (*EML4*) and anaplastic lymphoma kinase (*ALK*) gene fusions

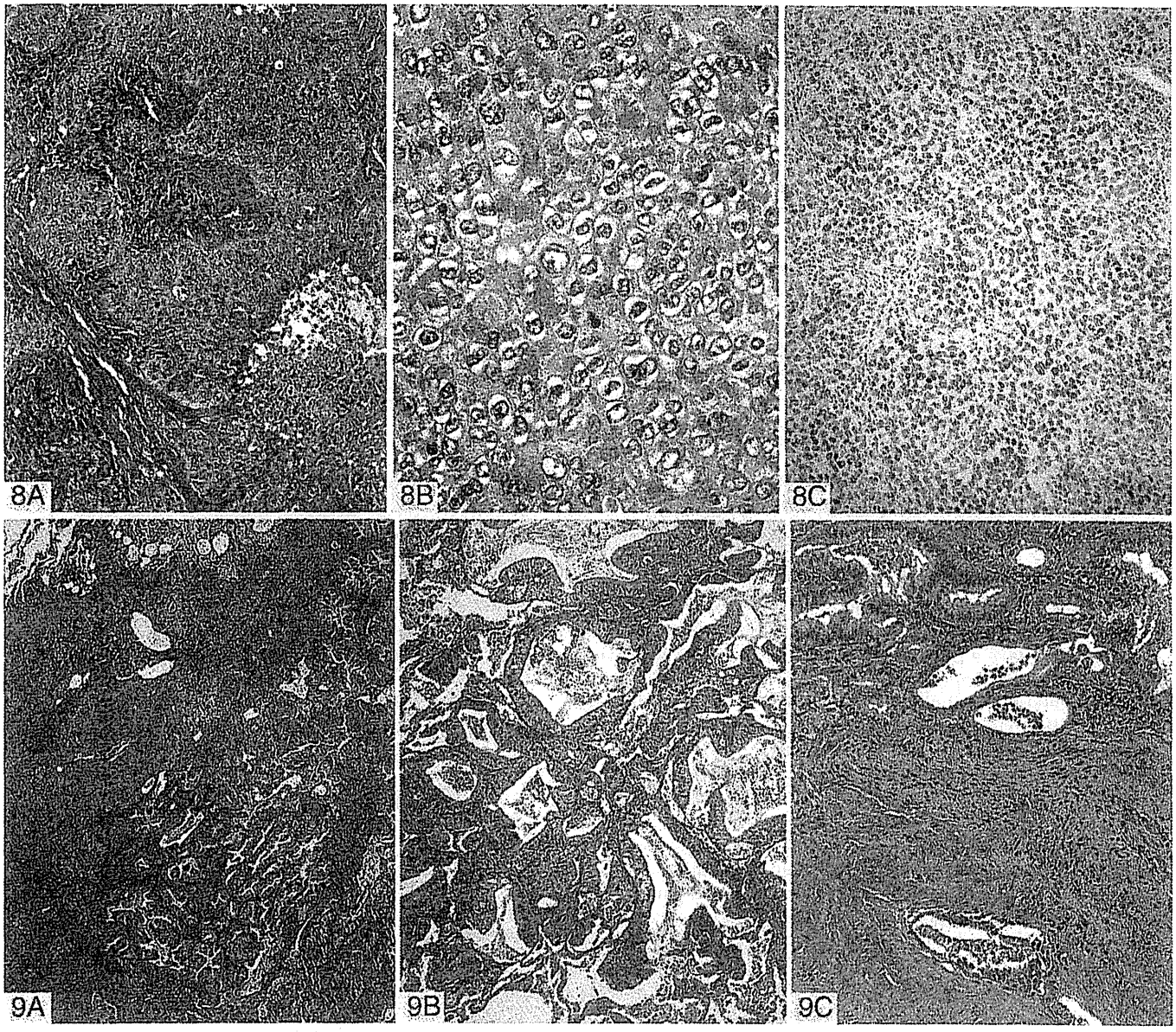

Figure 8. *Solid adenocarcinoma with mucin and pseudosquamous morphology. A, This tumor consists of sheets of tumor cells with abundant cytoplasm and mostly vesicular nuclei with several conspicuous nucleoli. Because this tumor had prominent eosinophilic cytoplasm, it was originally classified as squamous cell carcinoma. No acinar, papillary, or lepidic patterns are seen and there was no suggestion of mucin in tumor cell cytoplasm. B, The tumor showed foci of strong staining for intracytoplasmic mucin in numerous tumor cells. C, Thyroid transcription factor-1 (TTF-1) was diffusely and strongly positive. This tumor had an EGFR exon 19 deletion (hematoxylin-eosin, original magnification ×10 [A]; mucicarmine, original magnification ×40 [B]; TTF-1, original magnification ×20 [C]).*

Figure 9. *Invasive mucinous adenocarcinoma. A, This area of invasive mucinous adenocarcinoma demonstrates areas with lepidic, acinar, and papillary patterns. In addition, there is a fibrotic focus that contains invasive tumor with a desmoplastic stroma. B, The tumor consists of columnar cells filled with abundant mucin in the apical cytoplasm and shows small, basally oriented nuclei. This area shows mostly lepidic growth but also areas suggesting an acinar pattern. C, This photomicrograph highlights a focus of invasion with desmoplastic stroma from A. The invasive area shows an acinar pattern and the tumor cells show less cytoplasmic mucin (hematoxylin-eosin, original magnifications ×4 [A], ×10 [B], and ×20 [C]).*

(EML4-ALK).[113] Rather than diminishing the recognition of these features, this approach will now record any percentage (even <5%) of clear cell or signet ring features, whereas in the previous WHO classifications, the amount needed to be substantial, at the level of a histologic subtype, before it would be included in the diagnosis.

Rationale for Adding Enteric Adenocarcinoma.—Enteric adenocarcinoma is added to the classification to draw attention to this rare histologic type of primary lung adenocarcinoma, which can share some morphologic and immunohistochemical features with colorectal adenocarcinoma.[114] Owing to these similarities, clinical evaluation is needed to exclude a gastrointestinal primary tumor. It is not known if there are any distinctive clinical or molecular features.

Rationale for Maintaining Fetal Adenocarcinoma.—Fetal adenocarcinomas are maintained in this classification with the recognition that low-grade fetal adenocarcinomas are most commonly seen in the fourth decade of life with a slight female

Table 6. Difference Between Invasive Mucinous Adenocarcinoma and Nonmucinous Adenocarcinoma In Situ (AIS)/ Minimally Invasive Adenocarcinoma (MIA)/Lepidic-Predominant Adenocarcinoma (LPA)

Characteristics	Invasive Mucinous Adenocarcinoma (Formerly Mucinous BAC)	Nonmucinous AIS/MIA/LPA (Formerly Nonmucinous BAC)
Female, No. (%)	49/84 (58)[11,17,30,142,143]	101/140 (72)[11,17,30,142,143]
Smoker, No. (%)	39/87 (45)[11,17,30,142,144]	75/164 (46)[11,17,30,142,144]
Radiographic appearance	Majority consolidation; air bronchogram;[13] frequent multifocal and multilobar presentation[12–14,106,108,145,146]	Majority ground-glass attenuation[13,14,37,147–151]
Cell type	Mucin filled, columnar, and/or goblet[13,27,28,30,152]	Type II pneumocyte and/or Clara cell[13,27,28,30,152]
Immunophenotype		
CK7	Mostly positive[a] (+, ≈88%)[14,16,153–156]	Positive[a] (+, ≈98%)[14,16,153–156]
CK20	Positive[a] (+, ≈54%)[14,16,153–156]	Mostly negative[a] (+, ≈5%)[14,16,153–156]
TTF-1	Mostly negative[a] (+, ≈17%)[14,16,17,153,154,156,157]	Positive[a] (+, ≈67%)[14,16,17,153,154,156,157]
Genotype		
KRAS mutation	Frequent[a] (+, ≈76%)[14,15,106,158–160]	Uncommon[a] (+, ≈13%)[11,14,15,106,158–161]
EGFR mutation	Almost none[a] (+, ≈3%)[11,14,15,106,158–161]	Frequent[a] (+, ≈45%)[11,14,15,106,158–161]

Abbreviations: BAC, bronchioloalveolar carcinoma; CK, cytokeratin; TTF-1, thyroid transcription factor-1.

[a] Numbers represent the percentage of cases that are reported to be positive.

preponderance, whereas high-grade fetal adenocarcinomas are most commonly seen in elderly males, suggesting the 2 subtypes may have different oncogenic pathways.[115–117]

Histologic Features of Variant Subtypes

Invasive mucinous adenocarcinoma (formerly mucinous BAC) has a distinctive histologic appearance in which the tumor cells have a goblet or columnar cell morphology with abundant intracytoplasmic mucin (Figure 9, A through C). Nuclear atypia is usually inconspicuous or absent. Alveolar spaces often contain mucin. These tumors may show the same heterogeneous mixture of lepidic, acinar, papillary, micropapillary, and solid growth as in nonmucinous tumors (Figure 9, B and C). The clinical significance of reporting semiquantitative estimates of subtype percentages and the predominant histologic subtype, similar to nonmucinous adenocarcinomas, is not certain. When stromal invasion is seen, the malignant cells may show less cytoplasmic mucin and more atypia (Figure 9, C). These tumors differ from mucinous AIS and MIA by 1 or more of the following criteria: size (>3 cm), amount of invasion (>0.5 cm), multiple nodules, or lack of a circumscribed border with miliary spread into adjacent lung parenchyma.

There is a strong tendency for multicentric, multilobar, and bilateral lung involvement, which may reflect aerogenous spread. Mixtures of mucinous and nonmucinous tumors may rarely occur; if so, the percentage of invasive mucinous adenocarcinoma should be recorded in a comment. If there is at least 10% of each component, it should be classified as "mixed invasive mucinous and nonmucinous adenocarcinoma" with a description of the various components that comprise the tumor.

Invasive mucinous adenocarcinomas (formerly mucinous BAC) need to be distinguished from adenocarcinomas that produce mucin but lack the characteristic goblet cell or columnar cell morphology of the tumors that have historically been classified as mucinous BAC. When mucin is identified by light microscopy or mucin stains in adenocarcinomas that do not meet the above criteria, this feature should be reported in a comment after classifying the tumor according to the appropriate terminology and criteria proposed in this classification. This can be done by adding a descriptive phrase such as "with mucin production" or "with mucinous features," rather than the term *invasive mucinous adenocarcinoma*. Because of the multiple ways mucin can be expressed in lung adenocarcinomas, the specific wording "invasive mucinous adenocarcinoma" is important for this diagnosis.

Metastatic mucinous adenocarcinomas from sites such as the pancreas and ovary can appear morphologically identical to pulmonary invasive mucinous adenocarcinomas; therefore, clinical and radiologic correlation should be made to exclude primary tumors in these locations. Pancreatic mucinous adenocarcinomas are more likely to express cytokeratin (CK) 20 and mucin 2 (MUC2).[118] Metastatic colorectal adenocarcinomas often express caudal-related homeobox 2 (CDX-2) and CK20 with lack of CK7.

Pathology Recommendation 8.—For adenocarcinomas formerly classified as mucinous BAC, we recommend they be separated from the adenocarcinomas formerly classified as nonmucinous BAC and, depending on the extent of lepidic versus invasive growth, that they be classified as mucinous AIS, mucinous MIA, or for overtly invasive tumors, as "invasive mucinous adenocarcinoma" (weak recommendation, low-quality evidence).

Colloid adenocarcinoma shows abundant extracellular mucin in pools, which distend alveolar spaces and destroy their walls (Figure 10, A and B). The mucin pools contain clusters of mucin-secreting tumor cells, which may comprise only a small percentage of the total tumor volume (or area) and thus be inconspicuous (Figure 10, A).[119,120] The tumor cells may consist of goblet cells or other mucin-secreting cells and may form a single layer along fibrous septa (Figure 10, B). Colloid adenocarcinoma is found more often as a mixture with other adenocarcinoma histologic subtypes rather than as a pure pattern. A tumor is classified as a colloid adenocarcinoma when it is the predominant component; the percentages of other components should be recorded.[110] Cystic gross and or histologic features are included in the spectrum of colloid adenocarcinoma, but in most cases this is a focal feature. Cases previously reported as mucinous cystadenocarcinoma are extremely rare and now these should be classified as colloid adenocarcinoma with cystic changes. The cysts are filled with mucin, and lined by goblet or other mucin-secreting cells. The lining epithelium may be discontinuous and replaced with inflammation including a granulomatous reaction or gran-

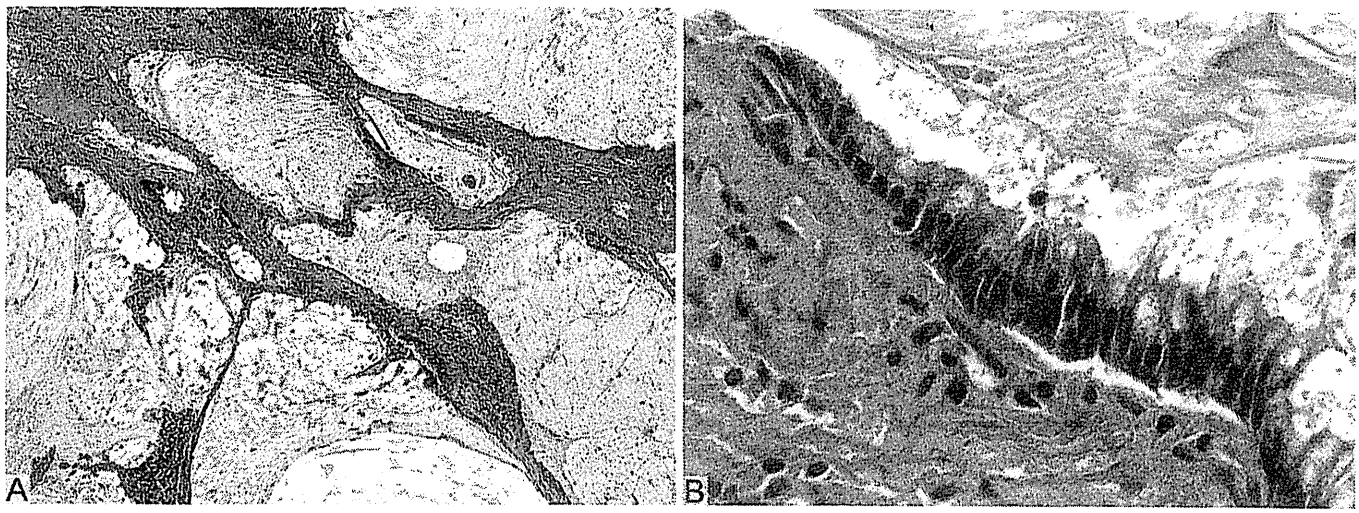

Figure 10. *Colloid adenocarcinoma. A,This tumor consists of abundant pools of mucin growing within and distending airspaces. Focally well-differentiated mucinous glandular epithelium grows along the surface of fibrous septa and within the pools of mucin. Tumor cells may be very inconspicuous. B, The surface of the fibrous wall is lined by well-differentiated cuboidal or columnar mucinous epithelium (hematoxylin-eosin, original magnifications ×10 [A] and ×40 [B]).*

ulation tissue. Nuclear atypia of the neoplastic epithelium is usually minimal.[121] Morphologically, this tumor may be fully indistinguishable from metastases from the appendix; clinical history should be very helpful.[122]

Fetal adenocarcinoma consists of glandular elements with tubules composed of glycogen-rich, nonciliated cells that resemble fetal lung tubules (Figure 11).[3] Subnuclear vacuoles are common and characteristic. Squamoid morules may be in the lumens. Most are low grade with a favorable outcome; high-grade tumors occur. When mixtures occur with other histologic subtypes, a feature that occurs more often in the high-grade tumors, the tumor should be classified according to the predominant component.[115] This tumor typically occurs in younger patients than do other adenocarcinomas. Uniquely, the low-grade fetal adenocarcinomas appear to be driven by mutations in the β-catenin gene and the epithelial cells express aberrant nuclear and cytoplasmic staining with this antibody by immunohistochemistry.[116,117,123] Nakatani et al[116,117] and Sekine et al[123] have suggested that upregulation of components in the WNT signaling pathway, such as β-catenin, are important in low-grade fetal adenocarcinomas, as well as in biphasic pulmonary blastomas. This is in contrast to the high-grade fetal adenocarcinomas, which appear to be distinct from the low-grade tumors.[116,117,123]

Enteric differentiation can occur in lung adenocarcinoma and when this component exceeds 50%, the tumor is classified as pulmonary adenocarcinoma with enteric differentiation. The enteric pattern shares morphologic and immunohistochemical features with colorectal adenocarcinoma.[114] In contrast to metastatic colorectal adenocarcinoma, these tumors are histologically heterogeneous with some component that resembles primary lung adenocarcinoma such as lepidic growth. Recording of the percentages of these other components may be useful. The enteric pattern consists of glandular and/or papillary structures, sometimes with a cribriform pattern (Figure 12, A), lined by tumor cells that are mostly tall columnar with nuclear pseudostratification, luminal necrosis, and prominent nuclear debris.[114] Poorly differentiated tumors may have a more solid pattern. These tumors show at least 1 immunohistologic marker of enteric differentiation (CDX-2, CK20, or MUC2) (Figure 12, B). Consistent positivity for CK7 and expression of TTF-1 in approximately half the cases help in the distinction from metastatic colorectal adenocarcinoma.[114,124] Cytokeratin 7–negative cases may occur.[125] CDX-2 is reduced or absent in most poorly differentiated colorectal carcinomas and more than half show the high-frequency microsatellite instability phenotype.[126] Although this type of tumor will rarely metastasize to the lung, since immunohistochemical detection of mismatch repair protein

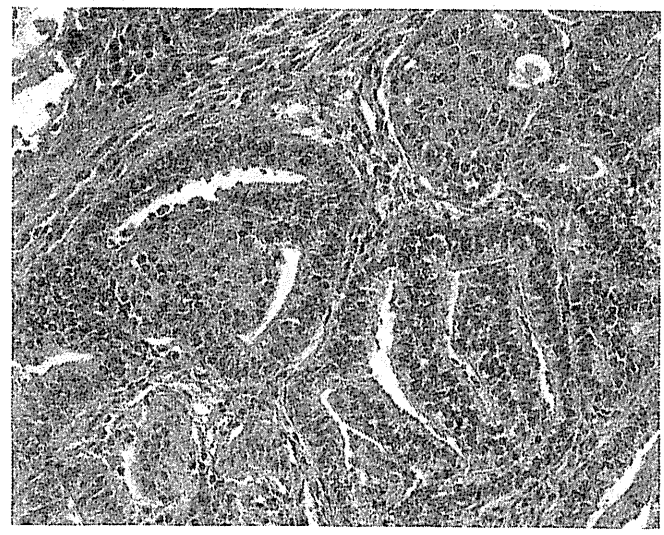

Figure 11. *Fetal adenocarcinoma consists of malignant glandular cells growing in tubules and papillary structures with endometrioid morphology. Some tumor cells have prominent clear cytoplasm, and squamoid morules are present (hematoxylin-eosin, original magnification ×20).*

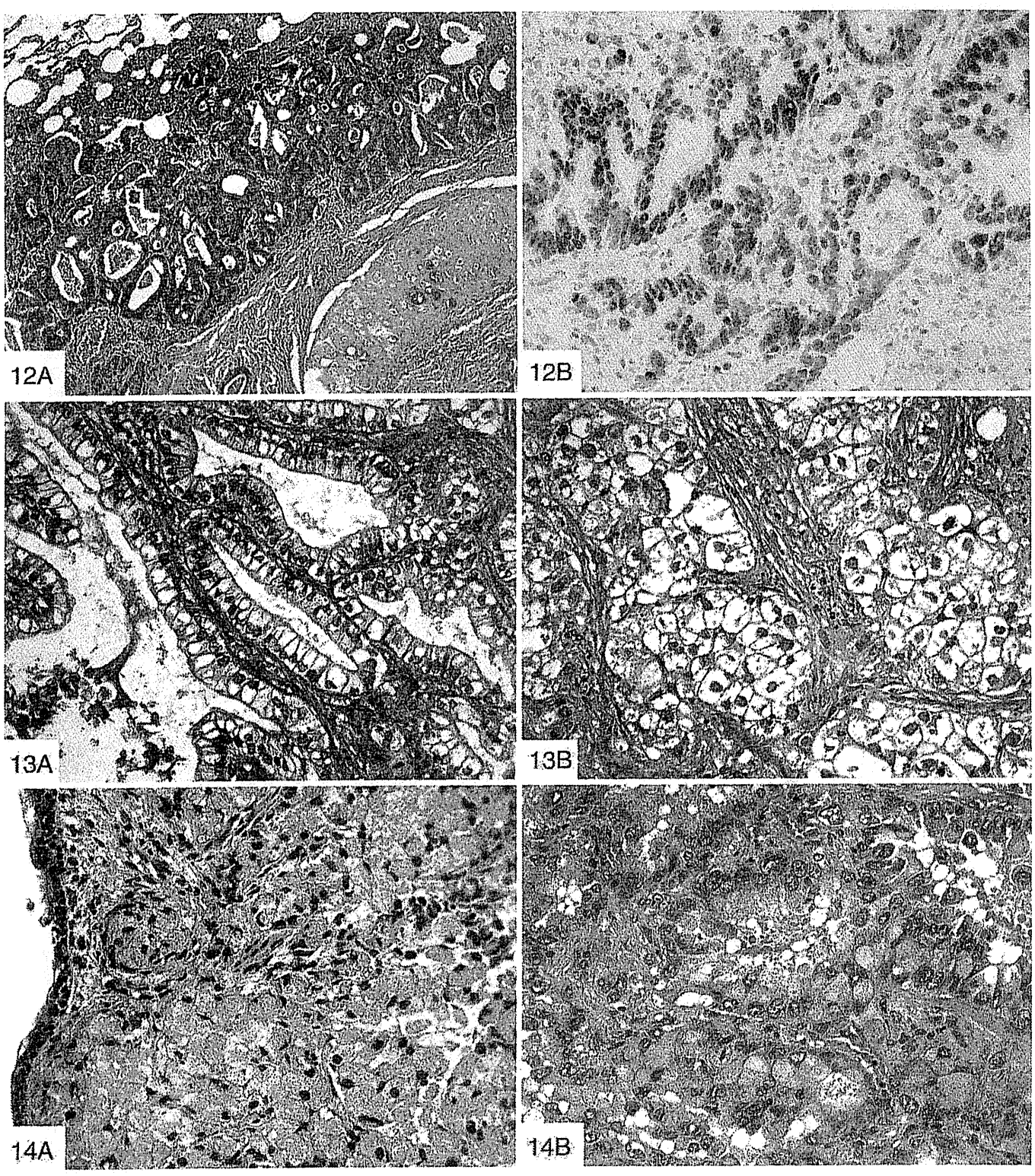

Figure 12. *Enteric adenocarcinoma. A, This tumor consists of an adenocarcinoma that morphologically resembles colonic adenocarcinoma with back-to-back angulated acinar structures. The tumor cells are cuboidal to columnar with nuclear pseudostratification. B, The tumor stains strongly for CDX-2 (hematoxylin-eosin, original magnification ×10 [A]; original magnification ×40 [B].*

Figure 13. *A, Acinar adenocarcinoma with clear cells. The cytoplasm in these tumor cells shows prominent clear cell features. B, Solid adenocarcinoma with clear cell features. The tumor cells in these solid nests have abundant clear cytoplasm (hematoxylin-eosin, original magnifications ×40 [A and B]).*

Figure 14. *Clear cell features: Signet ring features. A, Solid adenocarcinoma with signet ring features. This tumor consists of a uniform population of tumor cells with cytoplasm distended with abundant mucin, with many showing signet ring features. B, Acinar adenocarcinoma with signet ring features. Many tumor cells in this acinar pattern of adenocarcinoma have signet ring morphology (hematoxylin-eosin, original magnifications ×40 [A and B]).*

with antibodies for mutL homolog-1 (*MLH1*), mutS homologs 2 and 6 (*MSH2, MSH6*), and postmeiotic segregation increased 2 (*PMS2*) gives a predictive value that is virtually equivalent to microsatellite instability testing, this may be worth testing in selected cases as microsatellite instability in primary lung adenocarcinomas is extremely rare.[127] Primary lung adenocarcinomas that histologically resemble colorectal adenocarcinoma, but lack immunohistochemical markers of enteric differentiation, are probably better regarded as lung adenocarcinomas with *enteric morphology* rather than pulmonary adenocarcinoma with enteric differentiation.[128]

Signet Ring and Clear Cell Features

Both clear cell (Figure 13, A and B) and signet ring (Figure 14, A and B) features are regarded as cytologic features rather than primary histologic subtypes. They both occur most commonly in the solid component of lung adenocarcinomas (Figures 13, B, and 14, A), but they can also be seen in other patterns such as acinar (Figures 13, A, and 14, B), papillary, and micropapillary adenocarcinoma.[111,112] Therefore, these features should not be included in predominant subtype or the summary of percentages for comprehensive histologic subtyping, but rather they can be mentioned at the end of the diagnosis as "with signet ring features" or "with clear cell features," along with the estimated percentage of this cytologic change.

HISTOLOGIC GRADING

Unlike carcinomas of organs such as the breast, prostate, and kidney, there is no established grading system for lung adenocarcinoma in resection specimens. Since the effort to develop this new classification was begun, several studies have examined both architectural and nuclear approaches. While certain histologic subtypes are associated with favorable (lepidic pattern)[5] or unfavorable (solid, micropapillary)[6,9,10,129] prognosis, few articles have addressed grading across all histologic subtypes. Two major studies have addressed architectural grading using the single most predominant pattern[8] or the 2 most prominent patterns.[78] Both approaches have identified prognostically important subsets of lung adenocarcinoma. Nuclear grading has been evaluated in 3 studies, with two suggesting that nuclear size[130,131] and the other that cytologic atypia[129] were predictive of survival. A recent study[132] evaluated both nuclear and architectural grading in stage I lung adenocarcinomas. Although nuclear diameter, nuclear atypia, mitotic count, and atypical mitoses were significant predictors of recurrence in univariate analysis, in multivariate analysis only mitotic count had a significant independent association with risk of recurrence. Increased risk of recurrence was best predicted by a combined high architectural/mitotic grade after adjusting for clinical factors.[132] The impact of adding mitotic counts was greatest in tumors with intermediate architectural grade.[132] While these studies are promising, more validation studies are needed before a final grading system can be recommended for lung adenocarcinoma.

MOLECULAR-HISTOLOGIC CORRELATIONS

The molecular issues in lung adenocarcinoma are addressed in detail in the master classification document.[1] However, because of the importance of molecular histologic correlations, a few brief comments will be addressed. Unlike the specific genetic alterations seen in sarcomas, lymphomas, and leukemias, in lung cancer there are no histologic molecular correlations that are totally specific. Overall molecular, radiologic, and gene pathway correlations with adenocarcinoma subtypes are summarized in Table 7. The most robust histologic molecular correlation is with invasive mucinous adenocarcinoma, since a high percentage of these tumors have *KRAS* mutations and lack of *EGFR* mutations (Table 6). *EGFR* and *KRAS* mutations, as well as *ALK* rearrangement, can be seen in most of the invasive adenocarcinoma histologic subtypes. However, *EGFR* mutations are most often seen in association with nonmucinous adenocarcinomas that are lepidic or papillary predominant, and some report an association with a micropapillary pattern (Table 7). *KRAS* mutations are reported most often in tumors with a solid or micropapillary pattern and can be present in tumors producing extracellular mucin (Table 7). *ALK* rearrangement has been mostly associated with an acinar pattern, including a cribriform morphology, and with signet ring cell features, particularly those with TTF-1 and p63 coexpression.[133–136] Another point of interest is that nonsmoker-associated gene mutations, including *EGFR, EML4-ALK, BRAF,* and human epidermal growth factor receptor 2 (*HER2/neu*), are involved in a subset of adenocarcinomas with TTF-1 expression.[137]

With the emerging importance of molecular diagnostics to guide therapy, a multidisciplinary approach is needed to set a consistent strategy for obtaining and preserving tissue samples optimized to perform studies such as DNA sequence analysis, fluorescence in situ hybridization, and, in some settings, RNA-based studies. It is not yet possible to provide specific guidelines on how to do this in the current document because of the wide variation in infrastructure and expertise from one institution to another. If a portion of a sampled tumor is snap frozen for molecular studies, a few considerations exist for resection specimens. As most critical molecular studies can be performed from formalin-fixed, paraffin-embedded tissue, there is a need for frozen samples only for certain techniques such as comparative genomic hybridization and gene expression profiling. If frozen tissue is being obtained from tumors with lepidic-predominant tumors, for which AIS or MIA is in the differential diagnosis, efforts should be made to ascertain whether this frozen piece has an invasive component. The CT and gross appearance of the lesion should be considered to ensure a solid component is sampled in a tumor that appears part solid on CT. One approach is to perform a frozen section from the tissue saved for storage in a freezer. It is important to have a pathologist confirm the presence of tumor cells before performing molecular studies in the frozen tumor tissue samples.

RADIOLOGIC-HISTOLOGIC CORRELATIONS

There are settings in which pathologic assessment of lung adenocarcinomas can be greatly improved by correlation with radiologic findings. While review of CT reports may be informative, it is also helpful to have access to primary CT images in the frozen section and gross rooms, where pathology specimens are initially processed, and also at the time of review of histologic sections. Review of CT images may be valuable because they may give a better impression about the gross pathologic findings, which can be difficult to appreciate if tumors are removed by the surgeon in several pieces or if the tumor is difficult to identify on gross examination. In this sense, the CT is an extension of the

Table 7. Adenocarcinoma Histologic Subtypes, Molecular and Radiologic Associations

Histologic Subtype Predominant	Molecular Features	CT Scan Appearance	Gene Pathways Associated	Sources
Nonmucinous adenocarcinoma in situ and minimally invasive adenocarcinoma	TTF-1+ (100%); *EGFR* mutation never-smokers: 10%–30%; *KRAS* mutation smokers: 10%–30%	Ground-glass nodule, part-solid nodule	Not known	160, 162, 163, 164, 165
Lepidic (nonmucinous)	TTF-1+ (100%); *EGFR* mutation never-smokers: 10%–30%; *EGFR* amplification: 20%–50%; *KRAS* mutation smokers: 10%; *BRAF* mutations: 5%	Part-solid nodule; ground-glass nodule or solid nodule	Low cell cycle stimulatory; high *WNT*	6, 163, 164, 165, 166, 167, 168, 169, 170, 171
Papillary	TTF-1+ (90%–100%); *EGFR* mutation: 10%–30%; *EGFR* amplification: 20%–50%; *KRAS* mutation: 3% (lack of KRAS); *ERBB2* mutations: 3%; *TP53* mutations: 30%; *BRAF* mutations: 5%	Solid nodule	Low cell cycle stimulatory; high *EGFR*; high Notch	6, 79, 163, 166, 167, 168, 170, 172, 173, 174, 175
Acinar	TTF-1+ or –; *KRAS* mutation in smokers: 20%; *EGFR* mutations: <10% nonsmokers; *EGFR* amplification: 10%; *EML4/ALK* translocation: >5%; *TP53* mutations: 40%	Solid nodule	High *PDGF*; low *EGFR*; low angiogenesis	6, 79, 166, 176, 177
Micropapillary	*KRAS* mutations: 33%; *EGFR* mutations: 20%; *BRAF* mutations: 20%	Unknown	Unknown	6, 75, 171
Solid	TTF-1 (70%); MUC1 positive; *KRAS* mutation smokers: 10%–30%; *EGFR* mutation never-smokers: 10%–30%; *EGFR* amplification: 20%–50%; *EML4/ALK* translocation: >5%; *TP53* mutation: 50%; *LRP1B* mutations; *INHBA* mutations	Solid	High cell cycle stimulatory; high angiogenesis; high *JAK-STAT*; low Notch	6, 79, 166, 176, 177, 178, 179
Invasive mucinous adenocarcinoma	TTF-1 (0%–33% positive); *KRAS* mutation: 80%–100%; no *EGFR* mutation; MUC5+ MUC6+ MUC2+	Consolidation, air bronchograms; less often, ground-glass opacity	Not known	15, 91, 105, 153, 157, 159, 160, 175, 178, 180, 181

Abbreviations: CT, computed tomography; TTF-1, thyroid transcription factor-1.

gross pathologic assessment. There are 2 primary settings in which radiologic pathologic correlation is helpful: (1) in lepidic-predominant tumors (see "Radiologic-Pathologic Correlation for Tumor Size Assessment" above) and (2) if there are multiple tumors. In processing specimens with multiple nodules, review of the CT scan can also be helpful to be sure that each nodule is sampled.

IMPLICATIONS OF THIS CLASSIFICATION FOR TNM STAGING

There are several important implications of this new adenocarcinoma classification for staging that need to be considered for the next revision of the TNM classification. Importantly, we are not making official recommendations, as this can only be done by the International Union Against Cancer/American Joint Committee on Cancer TNM committees. However, we hope to stimulate investigators to study their case material with the intention of providing data that will allow these committees to determine whether official changes should be made in the 8th edition of the TNM classification. The changes relating to the concepts of AIS, MIA, and lepidic-predominant adenocarcinoma parallel classification criteria and terminology currently used in breast cancer,[138] but they would not be applicable to other histologic types of lung cancer. In addition, the comprehensive histologic subtyping approach to assessing invasive adenocarcinomas in this classification provides a useful approach to staging multiple adenocarcinomas.

Adenocarcinoma in situ would be classified as Tis. However, because carcinoma in situ (CIS) can occur with both lung squamous cell carcinoma and adenocarcinoma, these should be specified as Tis (squamous) or Tis (adenocarcinoma), similar to breast cancer where there is Tis (DCIS) for ductal CIS and Tis (LCIS) for lobular CIS.

Minimally invasive adenocarcinoma would be classified as T1mi, similar to microinvasive breast cancer, which is defined as an invasive carcinoma with no focus measuring greater than 1 mm; however, the size for MIA is not greater than 5 mm.

Also, similar to breast cancer, the size T factor for adenocarcinomas with an in situ or lepidic component may best predict prognosis according to the size of the invasive component only rather than the way it is currently practiced by including total tumor size inclusive of both the invasive and the lepidic or in situ components. In early-stage tumors, the tumor size T factor may need to be adjusted from total tumor size to the size of the invasive component only. Several publications in the literature[8,20,23] suggest invasive tumor size is an independent prognostic factor, and it may be a better predictor of prognosis than overall tumor size in lepidic predominant tumors. This needs to be tested radiologically and pathologically by comparing survival according to analysis of total tumor size (ground-glass opacity plus solid components by CT and invasive versus in situ/lepidic components by pathology) compared to only by the size of the solid or invasive component by CT and pathology examinations, respectively.

In addition, for multiple lung adenocarcinomas, comprehensive histologic subtyping can help in distinguishing intrapulmonary metastasis from synchronous or metachro-

nous primary tumors.[21] However, comprehensive histologic subtyping is only 1 tool that should be used to compare tumors, because valuable information can be obtained to address this problem from tumor cytologic characteristics and tumor stroma.[21] The role of molecular testing in this setting is promising, but needs further study.[22,139–141]

These concepts need to be tested vigorously in the next 5 years in both early- and advanced-stage lung adenocarcinoma to determine whether they are sufficiently robust to warrant changes in the 8th edition TNM classification.

References

1. Travis WD, Brambilla E, Noguchi M, et al. The New IASLC/ATS/ERS international multidisciplinary lung adenocarcinoma classification. *J Thoracic Oncol*. 2011;6(2):244–285.
2. Travis WD, Colby TV, Corrin B, Shimosato Y, Brambilla E; in collaboration with L.H. Sobin and pathologists from 14 countries. *Histological Typing of Lung and Pleural Tumors*. 3rd ed. Berlin, Germany: Springer; 1999.
3. Travis WD, Brambilla E, Müller-Hermelink HK, Harris CC. *Pathology and Genetics: Tumours of the Lung, Pleura, Thymus and Heart*. Lyon, France: IARC; 2004. *World Health Organization Classification of Tumours*; vol 10.
4. Travis WD, Brambilla E, Noguchi M, et al. Diagnosis of Lung Cancer in Small Biopsies and Cytology: Implications of the 2011 International Association for the Study of Lung Cancer/American Thoracic Society/European Respiratory Society Classificiation. *Arch Pathol Lab Med*. 2012;137(5):668–684.
5. Noguchi M, Morikawa A, Kawasaki M, et al. Small adenocarcinoma of the lung: histologic characteristics and prognosis. *Cancer*. 1995;75(12):2844–2852.
6. Motoi N, Szoke J, Riely GJ, et al. Lung adenocarcinoma: modification of the 2004 WHO mixed subtype to include the major histologic subtype suggests correlations between papillary and micropapillary adenocarcinoma subtypes, EGFR mutations and gene expression analysis. *Am J Surg Pathol*. 2008;32(6):810–827.
7. Morishita Y, Fukasawa M, Takeuchi M, et al. Small-sized adenocarcinoma of the lung: cytologic characteristics and clinical behavior. *Cancer*. 2001;93(2): 124–131.
8. Yoshizawa A, Motoi N, Riely GJ, et al. Impact of proposed IASLC/ATS/ERS classification of lung adenocarcinoma: prognostic subgroups and implications for further revision of staging based on analysis of 514 stage I cases. *Mod Pathol*. 2011;24(5):653–664.
9. Miyoshi T, Satoh Y, Okumura S, et al. Early-stage lung adenocarcinomas with a micropapillary pattern, a distinct pathologic marker for a significantly poor prognosis. *Am J Surg Pathol*. 2003;27(1):101–109.
10. Amin MB, Tamboli P, Merchant SH, et al. Micropapillary component in lung adenocarcinoma: a distinctive histologic feature with possible prognostic significance. *Am J Surg Pathol*. 2002;26(3):358–364.
11. Hata A, Katakami N, Fujita S, et al. Frequency of EGFR and KRAS mutations in Japanese patients with lung adenocarcinoma with features of the mucinous subtype of bronchioloalveolar carcinoma. *J Thorac Oncol*. 2010;5(8): 1197–1200.
12. Sawada E, Nambu A, Motosugi U, et al. Localized mucinous bronchioloalveolar carcinoma of the lung: thin-section computed tomography and fluorodeoxyglucose positron emission tomography findings. *Jpn J Radiol*. 2010; 28(4):251–258.
13. Lee HY, Lee KS, Han J, et al. Mucinous versus nonmucinous solitary pulmonary nodular bronchioloalveolar carcinoma: CT and FDG PET findings and pathologic comparisons. *Lung Cancer*. 2009;65(2):170–175.
14. Garfield DH, Cadranel J, West HL. Bronchioloalveolar carcinoma: the case for two diseases. *Clin Lung Cancer*. 2008;9(1):24–29.
15. Finberg KE, Sequist LV, Joshi VA, et al. Mucinous differentiation correlates with absence of EGFR mutation and presence of KRAS mutation in lung adenocarcinomas with bronchioloalveolar features. *J Mol Diagn*. 2007;9(3):320–326.
16. Goldstein NS, Thomas M. Mucinous and nonmucinous bronchioloalveolar adenocarcinomas have distinct staining patterns with thyroid transcription factor and cytokeratin 20 antibodies. *Am J Clin Pathol*. 2001;116(3):319–325.
17. Wislez M, Antoine M, Baudrin L, et al. Non-mucinous and mucinous subtypes of adenocarcinoma with bronchioloalveolar carcinoma features differ by biomarker expression and in the response to gefitinib. *Lung Cancer*. 2010; 68(2):185–191.
18. Aberle DR, Adams AM, Berg CD, et al. Reduced lung-cancer mortality with low-dose computed tomographic screening. *N Engl J Med*. 2011;365(5):395–340.
19. Mok TS. Personalized medicine in lung cancer: what we need to know. *Nat Rev Clin Oncol*. 2011;8(11):661–668.
20. Warth A, Muley T, Meister M, et al. Back to the roots: the novel histologic IASLC/ATS/ERS classification system of invasive pulmonary adenocarcinoma is a stage-independent predictor of survival. *J Clin Oncol*. 2012;30(13):1438–1446.
21. Girard N, Deshpande C, Lau C, et al. Comprehensive histologic assessment helps to differentiate multiple lung primary nonsmall cell carcinomas from metastases. *Am J Surg Pathol*. 2009;33(12):1752–1764.
22. Girard N, Ostrovnaya I, Lau C, et al. Genomic and mutational profiling to assess clonal relationships between multiple non-small cell lung cancers. *Clin Cancer Res*. 2009;15(16):5184–5190.
23. Tsutani Y, Miyata Y, Nakayama H, et al. Prognostic significance of using solid versus whole tumor size on high-resolution computed tomography for predicting pathologic malignant grade of tumors in clinical stage IA lung adenocarcinoma: A multicenter study. *J Thorac Cardiovasc Surg*. 2011;143(3): 607–612.
24. Schunemann HJ, Oxman AD, Brozek J, et al. Grading quality of evidence and strength of recommendations for diagnostic tests and strategies. *BMJ*. 2008; 336(7653):1106–1110.
25. Borczuk AC, Qian F, Kazeros A, et al. Invasive size is an independent predictor of survival in pulmonary adenocarcinoma. *Am J Surg Pathol*. 2009; 33(3):462–469.
26. Yim J, Zhu LC, Chiriboga L, et al. Histologic features are important prognostic indicators in early stages lung adenocarcinomas. *Mod Pathol*. 2007; 20(2):233–241.
27. Clayton F. Bronchioloalveolar carcinomas: cell types, patterns of growth, and prognostic correlates. *Cancer*. 1986;57:1555–1564.
28. Daly RC, Trastek VF, Pairolero PC, et al. Bronchoalveolar carcinoma: factors affecting survival. *Ann Thorac Surg*. 1991;51:368–376.
29. Goldstein NS, Mani A, Chmielewski G, Welsh R, Pursel S. Prognostic factors in T1 NO MO adenocarcinomas and bronchioloalveolar carcinomas of the lung. *Am J Clin Pathol*. 1999;112(3):391–402.
30. Manning JT Jr, Spjut HJ, Tschen JA. Bronchioloalveolar carcinoma: the significance of two histopathologic types. *Cancer*. 1984;54:525–534.
31. Riquet M, Foucault C, Berna P, et al. Prognostic value of histology in resected lung cancer with emphasis on the relevance of the adenocarcinoma subtyping. *Ann Thorac Surg*. 2006;81(6):1988–1995.
32. West HL, Franklin WA, McCoy J, et al. Gefitinib therapy in advanced bronchioloalveolar carcinoma: Southwest Oncology Group Study S0126. *J Clin Oncol*. 2006;24(12):1807–1813.
33. Garfield DH, Cadranel J. The importance of distinguishing mucinous and nonmucinous bronchioloalveolar carcinomas. *Lung*. 2009;187(3):207–208.
34. West HL, Garfield DH. Bronchioloalveolar carcinoma: not as easy as "BAC." *J Thorac Oncol*. 2009;4(9):1047–1048.
35. Gandara DR, Aberle D, Lau D, et al. Radiographic imaging of bronchioloalveolar carcinoma: screening, patterns of presentation and response assessment. *J Thorac Oncol*. 2006;1(9 suppl):S20–S26.
36. Raz DJ, He B, Rosell R, Jablons DM. Bronchioloalveolar carcinoma: a review. *Clin Lung Cancer*. 2006;7(5):313–322.
37. Travis WD, Garg K, Franklin WA, et al. Evolving concepts in the pathology and computed tomography imaging of lung adenocarcinoma and bronchioloalveolar carcinoma. *J Clin Oncol*. 2005;23(14):3279–3287.
38. Carey FA, Wallace WA, Fergusson RJ, Kerr KM, Lamb D. Alveolar atypical hyperplasia in association with primary pulmonary adenocarcinoma: a clinicopathological study of 10 cases. *Thorax*. 1992;47:1041–1043.
39. Weng SY, Tsuchiya E, Kasuga T, Sugano H. Incidence of atypical bronchioloalveolar cell hyperplasia of the lung: relation to histological subtypes of lung cancer. *Virchows Arch A Pathol Anat Histopathol*. 1992;420(6):463–471.
40. Nakanishi K. Alveolar epithelial hyperplasia and adenocarcinoma of the lung. *Arch Pathol Lab Med*. 1990;114(4):363–368.
41. Nakahara R, Yokose T, Nagai K, Nishiwaki Y, Ochiai A. Atypical adenomatous hyperplasia of the lung: a clinicopathological study of 118 cases including cases with multiple atypical adenomatous hyperplasia. *Thorax*. 2001; 56(4):302–305.
42. Miller RR. Bronchioloalveolar cell adenomas. *Am J Surg Pathol*. 1990; 14(10):904–912.
43. Nakayama H, Noguchi M, Tsuchiya R, Kodama T, Shimosato Y. Clonal growth of atypical adenomatous hyperplasia of the lung: cytofluorometric analysis of nuclear DNA content. *Mod Pathol*. 1990;3(3):314–320.
44. Niho S, Yokose T, Suzuki K, et al. Monoclonality of atypical adenomatous hyperplasia of the lung. *Am J Pathol*. 1999;154(1):249–254.
45. Sakamoto H, Shimizu J, Horio Y, et al. Disproportionate representation of KRAS gene mutation in atypical adenomatous hyperplasia, but even distribution of EGFR gene mutation from preinvasive to invasive adenocarcinomas. *J Pathol*. 2007;212(3):287–294.
46. Westra WH, Baas IO, Hruban RH, et al. K-ras oncogene activation in atypical alveolar hyperplasias of the human lung. *Cancer Res*. 1996;56(9):2224–2228.
47. Kohno T, Kakinuma R, Iwasaki M, et al. Association of CYP19A1 polymorphisms with risks for atypical adenomatous hyperplasia and bronchioloalveolar carcinoma in the lungs. *Carcinogenesis*. 2010;31(10):1794–1799.
48. Yoshida Y, Shibata T, Kokubu A, et al. Mutations of the epidermal growth factor receptor gene in atypical adenomatous hyperplasia and bronchioloalveolar carcinoma of the lung. *Lung Cancer*. 2005;50(1):1–8.
49. Yatabe Y, Kosaka T, Takahashi T, Mitsudomi T. EGFR mutation is specific for terminal respiratory unit type adenocarcinoma. *Am J Surg Pathol*. 2005;29(5): 633–639.
50. Kitamura H, Kameda Y, Nakamura N, et al. Atypical adenomatous hyperplasia and bronchoalveolar lung carcinoma: analysis by morphometry and the expressions of p53 and carcinoembryonic antigen. *Am J Surg Pathol*. 1996; 20(5):553–562.
51. Takamochi K, Ogura T, Suzuki K, et al. Loss of heterozygosity on chromosomes 9q and 16p in atypical adenomatous hyperplasia concomitant with adenocarcinoma of the lung. *Am J Pathol*. 2001;159(5):1941–1948.
52. Licchesi JD, Westra WH, Hooker CM, Herman JG. Promoter hypermethylation of hallmark cancer genes in atypical adenomatous hyperplasia of the lung. *Clin Cancer Res*. 2008;14(9):2570–2578.

53. Nakanishi K, Kawai T, Kumaki F, et al. Expression of human telomerase RNA component and telomerase reverse transcriptase mRNA in atypical adenomatous hyperplasia of the lung. *Hum Pathol.* 2002;33(7):697–702.
54. Seki N, Takasu T, Mandai K, et al. Expression of eukaryotic initiation factor 4E in atypical adenomatous hyperplasia and adenocarcinoma of the human peripheral lung. *Clin Cancer Res.* 2002;8(10):3046–3053.
55. Licchesi JD, Westra WH, Hooker CM, et al. Epigenetic alteration of Wnt pathway antagonists in progressive glandular neoplasia of the lung. *Carcinogenesis.* 2008;29(5):895–904.
56. Kerr KM, MacKenzie SJ, Ramasami S, et al. Expression of FHIT, cell adhesion molecules and matrix metalloproteinases in atypical adenomatous hyperplasia and pulmonary adenocarcinoma. *J Pathol.* 2004;203(2):638–644.
57. Maeshima AM, Tochigi N, Yoshida A, et al. Clinicopathologic analysis of multiple (five or more) atypical adenomatous hyperplasias (AAHs) of the lung: evidence for the AAH-adenocarcinoma sequence. *J Thorac Oncol.* 2010;5(4):466–471.
58. Mori M, Rao SK, Popper HH, Cagle PT, Fraire AE. Atypical adenomatous hyperplasia of the lung: a probable forerunner in the development of adenocarcinoma of the lung. *Mod Pathol.* 2001;14(2):72–84.
59. Kitamura H, Kameda Y, Ito T, Hayashi H. Atypical adenomatous hyperplasia of the lung. Implications for the pathogenesis of peripheral lung adenocarcinoma. *Am J Clin Pathol.* 1999;111(5):610–622.
60. Koga T, Hashimoto S, Sugio K, et al. Lung adenocarcinoma with bronchioloalveolar carcinoma component is frequently associated with foci of high-grade atypical adenomatous hyperplasia. *Am J Clin Pathol.* 2002;117(3):464–470.
61. Watanabe S, Watanabe T, Arai K, et al. Results of wedge resection for focal bronchioloalveolar carcinoma showing pure ground-glass attenuation on computed tomography. *Ann Thorac Surg.* 2002;73(4):1071–1075.
62. Sakurai H, Dobashi Y, Mizutani E, et al. Bronchioloalveolar carcinoma of the lung 3 centimeters or less in diameter: a prognostic assessment. *Ann Thorac Surg.* 2004;78(5):1728–1733.
63. Vazquez M, Carter D, Brambilla E, et al. Solitary and multiple resected adenocarcinomas after CT screening for lung cancer: histopathologic features and their prognostic implications. *Lung Cancer.* 2009;64(2):148–154.
64. Yoshida J, Nagai K, Yokose T, et al. Limited resection trial for pulmonary ground-glass opacity nodules: fifty-case experience. *J Thorac Cardiovasc Surg.* 2005;129(5):991–996.
65. Yamato Y, Tsuchida M, Watanabe T, et al. Early results of a prospective study of limited resection for bronchioloalveolar adenocarcinoma of the lung. *Ann Thorac Surg.* 2001;71(3):971–974.
66. Yamada S, Kohno T. Video-assisted thoracic surgery for pure ground-glass opacities 2 cm or less in diameter. *Ann Thorac Surg.* 2004;77(6):1911–1915.
67. Koike T, Togashi K, Shirato T, et al. Limited resection for noninvasive bronchioloalveolar carcinoma diagnosed by intraoperative pathologic examination. *Ann Thorac Surg.* 2009;88(4):1106–1111.
68. Maeshima AM, Tochigi N, Yoshida A, et al. Histological scoring for small lung adenocarcinomas 2 cm or less in diameter: a reliable prognostic indicator. *J Thorac Oncol.* 2010;5(3):333–339.
69. Lester SC, Bose S, Chen YY, et al. Protocol for the examination of specimens from patients with invasive carcinoma of the breast. *Arch Pathol Lab Med.* 2009;133(10):1515–1538.
70. Sakurai H, Maeshima A, Watanabe S, et al. Grade of stromal invasion in small adenocarcinoma of the lung: histopathological minimal invasion and prognosis. *Am J Surg Pathol.* 2004;28(2):198–206.
71. Suzuki K, Asamura H, Kusumoto M, Kondo H, Tsuchiya R. "Early" peripheral lung cancer: prognostic significance of ground glass opacity on thin-section computed tomographic scan. *Ann Thorac Surg.* 2002;74(5):1635–1639.
72. Oka S, Hanagiri T, Uramoto H, et al. Surgical resection for patients with mucinous bronchioloalveolar carcinoma. *Asian J Surg.* 2010;33(2):89–93.
73. Hammond ME, Hayes DF, Dowsett M, et al. American Society of Clinical Oncology/College of American Pathologists guideline recommendations for immunohistochemical testing of estrogen and progesterone receptors in breast cancer (unabridged version). *Arch Pathol Lab Med.* 2010;134(7):e48–e72.
74. Lindeman N, Cagle P, Ladanyi M. CAP/IASLC/AMP lung cancer biomarkers guideline. *Arch Pathol Lab Med.* 2012. In press.
75. De Oliveira Duarte AR, Nikiforova MN, Yousem SA. Micropapillary lung adenocarcinoma: EGFR, K-ras, and BRAF mutational profile. *Am J Clin Pathol.* 2009;131(5):694–700.
76. Nakamura Y, Niki T, Goto A, et al. c-Met activation in lung adenocarcinoma tissues: an immunohistochemical analysis. *Cancer Sci.* 2007;98(7):1006–1013.
77. Yoshizawa A, Sumiyoshi S, Moreira AL, Travis WD. Validation of the IASLC/ATS/ERS lung adenocarcinoma (ADC) classification and use of comprehensive histologic subtyping (CHS) for architectural grading in 432 Japanese patients. *Mod Pathol.* 2011;24(1S):429A.
78. Sica G, Yoshizawa A, Sima CS, et al. A grading system of lung adenocarcinomas based on histologic pattern is predictive of disease recurrence in stage I tumors. *Am J Surg Pathol.* 2010;34(8):1155–1162.
79. Ding L, Getz G, Wheeler DA, et al. Somatic mutations affect key pathways in lung adenocarcinoma. *Nature.* 2008;455(7216):1069–1075.
80. Shedden K, Taylor JM, Enkemann SA, et al. Gene expression-based survival prediction in lung adenocarcinoma: a multi-site, blinded validation study. *Nat Med.* 2008;14(8):822–827.
81. Sholl LM, Yeap BY, Iafrate AJ, et al. Lung adenocarcinoma with EGFR amplification has distinct clinicopathologic and molecular features in never-smokers. *Cancer Res.* 2009;69(21):8341–8348.
82. Dacic S, Shuai Y, Yousem S, Ohori P, Nikiforova M. Clinicopathological predictors of EGFR/KRAS mutational status in primary lung adenocarcinomas. *Mod Pathol.* 2010;23(2):159–168.
83. Kim YH, Ishii G, Goto K, et al. Dominant papillary subtype is a significant predictor of the response to gefitinib in adenocarcinoma of the lung. *Clin Cancer Res.* 2004;10(21):7311–7317.
84. Russell PA, Wainer Z, Wright GM, et al. Does lung adenocarcinoma subtype predict patient survival: a clinicopathologic study based on the new International Association for the Study of Lung Cancer/American Thoracic Society/European Respiratory Society international multidisciplinary lung adenocarcinoma classification. *J Thorac Oncol.* 2011;6(9):1496–1504.
85. Thunnissen FB, Beasley MB, Borczuk A, et al. Reproducibility of histopathological subtypes in pulmonary adenocarcinoma. *Mod Pathol.* 2012;25:e pub ahead of print.
86. Warth A, Stenzinger A, von Brunneck A-C, et al. Interobserver variability in the application of the novel IASLC/ATS/ERS Classification. *Eur Resp J.* 2012. In press.
87. Kadota K, Suzuki K, D'Angelo SP, et al. Validation of the proposed IASLC/American Thoracic Society (ATS)/European Respiratory Society (ERS) international multidisciplinary classification of lung adenocarcinoma (ADC). *J Thorac Oncol.* 2011;6(6 suppl 2):S286.
88. Kadota K, Suzuki K, Yoshizawa A, et al. Clinicopathologic characteristics of adenocarcinoma in situ (AIS), minimally invasive adenocarcinoma (MIA) and lepidic predominant (LPD) adenocarcinoma of the lung (LAC): Memorial Sloan-Kettering Cancer Center Experience. *J Thorac Oncol.* 2011;6(6 suppl 2):S287.
89. Shim HS, Lee da H, Park EJ, Kim SH. Histopathologic characteristics of lung adenocarcinomas with epidermal growth factor receptor mutations in the International Association for the Study of Lung Cancer/American Thoracic Society/European Respiratory Society lung adenocarcinoma classification. *Arch Pathol Lab Med.* 2011;135(10):1329–1334.
90. Sterlacci W, Savic S, Schmid T, et al. Tissue-sparing application of the newly proposed IASLC/ATS/ERS classification of adenocarcinoma of the lung shows practical diagnostic and prognostic impact. *Am J Clin Pathol.* 2012;137(6):946–956.
91. Lee HY, Han J, Lee KS, et al. Lung adenocarcinoma as a solitary pulmonary nodule: prognostic determinants of CT, PET, and histopathologic findings. *Lung Cancer.* 2009;66(3):379–385.
92. Lin DM, Ma Y, Zheng S, et al. Prognostic value of bronchioloalveolar carcinoma component in lung adenocarcinoma. *Histol Histopathol.* 2006;21(6):627–632.
93. Yokose T, Suzuki K, Nagai K, et al. Favorable and unfavorable morphological prognostic factors in peripheral adenocarcinoma of the lung 3 cm or less in diameter. *Lung Cancer.* 2000;29(3):179–188.
94. Okudela K, Woo T, Mitsui H, et al. Proposal of an improved histological sub-typing system for lung adenocarcinoma—significant prognostic values for stage I disease. *Int J Clin Exp Pathol.* 2010;3(4):348–366.
95. Silver SA, Askin FB. True papillary carcinoma of the lung: a distinct clinicopathologic entity. *Am J Surg Pathol.* 1997;21(1):43–51.
96. Hoshi R, Tsuzuku M, Horai T, Ishikawa Y, Satoh Y. Micropapillary clusters in early-stage lung adenocarcinomas: a distinct cytologic sign of significantly poor prognosis. *Cancer.* 2004;102(2):81–86.
97. Kamiya K, Hayashi Y, Douguchi J, et al. Histopathological features and prognostic significance of the micropapillary pattern in lung adenocarcinoma. *Mod Pathol.* 2008;21(8):992–1001.
98. Kawakami T, Nabeshima K, Hamasaki M, et al. Small cluster invasion: a possible link between micropapillary pattern and lymph node metastasis in pT1 lung adenocarcinomas. *Virchows Arch.* 2009;454(1):61–70.
99. Kuroda N, Hamaguchi N, Takeuchi E, et al. Lung adenocarcinoma with a micropapillary pattern: a clinicopathological study of 25 cases. *APMIS.* 2006;114(5):381–385.
100. Maeda R, Isowa N, Onuma H, et al. Lung adenocarcinomas with micropapillary components. *Gen Thorac Cardiovasc Surg.* 2009;57(10):534–539.
101. Makimoto Y, Nabeshima K, Iwasaki H, et al. Micropapillary pattern: a distinct pathological marker to subclassify tumours with a significantly poor prognosis within small peripheral lung adenocarcinoma (</=20 mm) with mixed bronchioloalveolar and invasive subtypes (Noguchi's type C tumours). *Histopathology.* 2005;46(6):677–684.
102. Sanchez-Mora N, Presmanes MC, Monroy V, et al. Micropapillary lung adenocarcinoma: a distinctive histologic subtype with prognostic significance. Case series. *Hum Pathol.* 2008;39(3):324–330.
103. Tsutsumida H, Nomoto M, Goto M, et al. A micropapillary pattern is predictive of a poor prognosis in lung adenocarcinoma, and reduced surfactant apoprotein A expression in the micropapillary pattern is an excellent indicator of a poor prognosis. *Mod Pathol.* 2007;20(6):638–647.
104. Bishop JA, Teruya-Feldstein J, Westra WH, et al. p40 (DeltaNp63) is superior to p63 for the diagnosis of pulmonary squamous cell carcinoma. *Mod Pathol.* 2012;25(3):405–415.
105. Awaya H, Takeshima Y, Yamasaki M, Inai K. Expression of MUC1, MUC2, MUC5AC, and MUC6 in atypical adenomatous hyperplasia, bronchioloalveolar carcinoma, adenocarcinoma with mixed subtypes, and mucinous bronchioloalveolar carcinoma of the lung. *Am J Clin Pathol.* 2004;121(5):644–653.

106. Casali C, Rossi G, Marchioni A, et al. A single institution-based retrospective study of surgically treated bronchioloalveolar adenocarcinoma of the lung: clinicopathologic analysis, molecular features, and possible pitfalls in routine practice. *J Thorac Oncol.* 2010;5(6):830–836.
107. Copin MC, Buisine MP, Leteurtre E, et al. Mucinous bronchioloalveolar carcinomas display a specific pattern of mucin gene expression among primary lung adenocarcinomas. *Hum Pathol.* 2001;32(3):274–281.
108. Miyake H, Matsumoto A, Terada A, et al. Mucin-producing tumor of the lung: CT findings. *J Thorac Imaging.* 1995;10(2):96–98.
109. Sato K, Ueda Y, Shikata H, Katsuda S. Bronchioloalveolar carcinoma of mixed mucinous and nonmucinous type: immunohistochemical studies and mutation analysis of the p53 gene. *Pathol Res Pract.* 2006;202(10):751–756.
110. Gaeta M, Blandino A, Scribano E, et al. Mucinous cystadenocarcinoma of the lung: CT-pathologic correlation in three cases. *J Comput Assist Tomogr.* 1999; 23(4):641–643.
111. Cohen PR, Yoshizawa A, Motoi N, et al. Signet ring cell features (SRCF) in lung adenocarcinoma: a cytologic feature or a histologic subtype? *Mod Pathol.* 2010;23(2):400A.
112. Deshpande CG, Yoshizawa A, Motoi N, et al. Clear cell change in lung adenocarcinoma: a cytologic change rather than a histologic variant. *Mod Pathol.* 2009;22(1S):352A.
113. Rodig SJ, Mino-Kenudson M, Dacic S, et al. Unique clinicopathologic features characterize ALK-rearranged lung adenocarcinoma in the western population. *Clin Cancer Res.* 2009;15(16):5216–5213.
114. Inamura K, Satoh Y, Okumura S, et al. Pulmonary adenocarcinomas with enteric differentiation: histologic and immunohistochemical characteristics compared with metastatic colorectal cancers and usual pulmonary adenocarcinomas. *Am J Surg Pathol.* 2005;29(5):660–665.
115. Nakatani Y, Kitamura H, Inayama Y, et al. Pulmonary adenocarcinomas of the fetal lung type: a clinicopathologic study indicating differences in histology, epidemiology, and natural history of low-grade and high-grade forms. *Am J Surg Pathol.* 1998;22(4):399–411.
116. Nakatani Y, Masudo K, Miyagi Y, et al. Aberrant nuclear localization and gene mutation of beta-catenin in low-grade adenocarcinoma of fetal lung type: up-regulation of the Wnt signaling pathway may be a common denominator for the development of tumors that form morules. *Mod Pathol.* 2002;15(6):617–624.
117. Nakatani Y, Miyagi Y, Takemura T, et al. Aberrant nuclear/cytoplasmic localization and gene mutation of beta-catenin in classic pulmonary blastoma: beta-catenin immunostaining is useful for distinguishing between classic pulmonary blastoma and a blastomatoid variant of carcinosarcoma. *Am J Surg Pathol.* 2004;28(7):921–927.
118. Chu PG, Chung L, Weiss LM, Lau SK. Determining the site of origin of mucinous adenocarcinoma: an immunohistochemical study of 175 cases. *Am J Surg Pathol.* 2011;35(12):1830–1836.
119. Moran CA, Hochholzer L, Fishback N, Travis WD, Koss MN. Mucinous (so-called colloid) carcinomas of lung. *Mod Pathol.* 1992;5(6):634–638.
120. Rossi G, Murer B, Cavazza A, et al. Primary mucinous (so-called colloid) carcinomas of the lung: a clinicopathologic and immunohistochemical study with special reference to CDX-2 homeobox gene and MUC2 expression. *Am J Surg Pathol.* 2004;28(4):442–452.
121. Gao ZH, Urbanski SJ. The spectrum of pulmonary mucinous cystic neoplasia: a clinicopathologic and immunohistochemical study of ten cases and review of literature. *Am J Clin Pathol.* 2005;124(1):62–70.
122. Geisinger KR, Levine EA, Shen P, Bradley RF. Pleuropulmonary involvement in pseudomyxoma peritonei: morphologic assessment and literature review. *Am J Clin Pathol.* 2007;127(1):135–143.
123. Sekine S, Shibata T, Matsuno Y, et al. Beta-catenin mutations in pulmonary blastomas: association with morule formation. *J Pathol.* 2003; 200(2):214–221.
124. Li HC, Schmidt L, Greenson JK, Chang AC, Myers JL. Primary pulmonary adenocarcinoma with intestinal differentiation mimicking metastatic colorectal carcinoma: case report and review of literature. *Am J Clin Pathol.* 2009;131(1): 129–133.
125. Hatanaka K, Tsuta K, Watanabe K, Sugino K, Uekusa T. Primary pulmonary adenocarcinoma with enteric differentiation resembling metastatic colorectal carcinoma: a report of the second case negative for cytokeratin 7. *Pathol Res Pract.* 2011;207(3):188–191.
126. Hinoi T, Tani M, Lucas PC, et al. Loss of CDX2 expression and microsatellite instability are prominent features of large cell minimally differentiated carcinomas of the colon. *Am J Pathol.* 2001;159(6):2239–2248.
127. Shia J. Immunohistochemistry versus microsatellite instability testing for screening colorectal cancer patients at risk for hereditary nonpolyposis colorectal cancer syndrome, part I: the utility of immunohistochemistry. *J Mol Diagn.* 2008; 10(4):293–300.
128. Yousem SA. Pulmonary intestinal-type adenocarcinoma does not show enteric differentiation by immunohistochemical study. *Mod Pathol.* 2005;18(6): 816–821.
129. Barletta JA, Yeap BY, Chirieac LR. Prognostic significance of grading in lung adenocarcinoma. *Cancer.* 2010;116(3):659–669.
130. Nakazato Y, Minami Y, Kobayashi H, et al. Nuclear grading of primary pulmonary adenocarcinomas: correlation between nuclear size and prognosis. *Cancer.* 2010;116(8):2011–2019.
131. Petersen I, Kotb WF, Friedrich KH, et al. Core classification of lung cancer: correlating nuclear size and mitoses with ploidy and clinicopathological parameters. *Lung Cancer.* 2009;65(3):312–318.
132. Kadota K, Suzuki K, Kachala SS, et al. Mitotic count is a predictor of recurrence in stage I lung adenocarcinoma generating a combined architectural and mitotic grading system. *Mod Pathol.* 2012;25(8):1117–1127.
133. Inamura K, Takeuchi K, Togashi Y, et al. EML4-ALK fusion is linked to histological characteristics in a subset of lung cancers. *J Thorac Oncol.* 2008;3(1): 13–17.
134. Yoshida A, Tsuta K, Watanabe SI, et al. Frequent ALK rearrangement and TTF-1/p63 co-expression in lung adenocarcinoma with signet-ring cell component. *Lung Cancer.* 2010;72(3):309–315.
135. McLeer-Florin A, Moro-Sibilot D, Melis A, et al. Dual IHC and FISH Testing for ALK Gene Rearrangement in Lung Adenocarcinomas in a Routine Practice: A French Study. *J Thorac Oncol.* 2011;7(2):348–354.
136. Mino-Kenudson M, Chirieac LR, Law K, et al. A novel, highly sensitive antibody allows for the routine detection of ALK-rearranged lung adenocarcinomas by standard immunohistochemistry. *Clin Cancer Res.* 2010;16(5):1561–1571.
137. Yatabe Y. EGFR mutations and the terminal respiratory unit. *Cancer Metastasis Rev.* 2010;29(1):23–36.
138. Hayes DF, Allred C, Anderson BO, et al. Breast. In: AJCC Cancer Staging Manual 7th Edition, Edge SB, Byrd DR, Compton CC, et al, eds. New York, NY: Springer; 2009.
139. Girard N, Deshpande C, Azzoli CG, et al. Use of epidermal growth factor receptor/Kirsten rat sarcoma 2 viral oncogene homolog mutation testing to define clonal relationships among multiple lung adenocarcinomas: comparison with clinical guidelines. *Chest.* 2010;137(1):46–52.
140. Iwata T, Sugio K, Uramoto H, et al. Detection of EGFR and K-ras mutations for diagnosis of multiple lung adenocarcinomas. *Front Biosci.* 2011;17: 2961–2969.
141. Chung JH, Choe G, Jheon S, et al. Epidermal growth factor receptor mutation and pathologic-radiologic correlation between multiple lung nodules with ground-glass opacity differentiates multicentric origin from intrapulmonary spread. *J Thorac Oncol.* 2009;4(12):1490–1495.
142. Yatabe Y, Mitsudomi T. Epidermal growth factor receptor mutations in lung cancers. *Pathol Int.* 2007;57(5):233–244.
143. Holst VA, Finkelstein S, Yousem SA. Bronchioloalveolar adenocarcinoma of lung: monoclonal origin for multifocal disease. *Am J Surg Pathol.* 1998;22(11): 1343–1350.
144. Furak J, Trojan I, Szoke T, et al. Bronchioloalveolar lung cancer: occurrence, surgical treatment and survival. *Eur J Cardiothorac Surg.* 2003; 23(5):818–823.
145. Akira M, Atagi S, Kawahara M, Iuchi K, Johkoh T. High-resolution CT findings of diffuse bronchioloalveolar carcinoma in 38 patients. *AJR Am J Roentgenol.* 1999;173(6):1623–1629.
146. Tateishi U, Muller NL, Johkoh T, et al. Mucin-producing adenocarcinoma of the lung: thin-section computed tomography findings in 48 patients and their effect on prognosis. *J Comput Assist Tomogr.* 2005;29(3):361–368.
147. Yabuuchi H, Murayama S, Murakami J, et al. High-resolution CT characteristics of poorly differentiated adenocarcinoma of the peripheral lung: comparison with well differentiated adenocarcinoma. *Radiat Med.* 2000;18(6): 343–347.
148. Aoki T, Tomoda Y, Watanabe H, et al. Peripheral lung adenocarcinoma: correlation of thin-section CT findings with histologic prognostic factors and survival. *Radiology.* 2001;220(3):803–809.
149. Kodama K, Higashiyama M, Yokouchi H, et al. Natural history of pure ground-glass opacity after long-term follow-up of more than 2 years. *Ann Thorac Surg.* 2002;73(2):386–392.
150. Im JG, Han MC, Yu EJ, et al. Lobar bronchioloalveolar carcinoma: "angiogram sign" on CT scans. *Radiology.* 1990;176(3):749–753.
151. Nagao M, Murase K, Yasuhara Y, et al. Measurement of localized ground-glass attenuation on thin-section computed tomography images: correlation with the progression of bronchioloalveolar carcinoma of the lung. *Invest Radiol.* 2002; 37(12):692–697.
152. Clayton F. The spectrum and significance of bronchioloalveolar carcinomas. *Pathol Annu.* 1988;23(pt 2):361–394.
153. Lau SK, Desrochers MJ, Luthringer DJ. Expression of thyroid transcription factor-1, cytokeratin 7, and cytokeratin 20 in bronchioloalveolar carcinomas: an immunohistochemical evaluation of 67 cases. *Mod Pathol.* 2002;15(5):538–542.
154. Sarantopoulos GP, Gui D, Shintaku P, et al. Immunohistochemical analysis of lung carcinomas with pure or partial bronchioloalveolar differentiation. *Arch Pathol Lab Med.* 2004;128(4):406–414.
155. Shah RN, Badve S, Papreddy K, et al. Expression of cytokeratin 20 in mucinous bronchioloalveolar carcinoma. *Hum Pathol.* 2002;33(9):915–920.
156. Simsir A, Wei XJ, Yee H, Moreira A, Cangiarella J. Differential expression of cytokeratins 7 and 20 and thyroid transcription factor-1 in bronchioloalveolar carcinoma: an immunohistochemical study in fine-needle aspiration biopsy specimens. *Am J Clin Pathol.* 2004;121(3):350–357.
157. Saad RS, Liu YL, Han H, Landreneau RJ, Silverman JF. Prognostic significance of thyroid transcription factor-1 expression in both early-stage conventional adenocarcinoma and bronchioloalveolar carcinoma of the lung. *Hum Pathol.* 2004;35(1):3–7.
158. Maeshima A, Sakamoto M, Hirohashi S. Mixed mucinous-type and non-mucinous-type adenocarcinoma of the lung: immunohistochemical examination and K- ras gene mutation. *Virchows Arch.* 2002;440(6):598–603.
159. Marchetti A, Buttitta F, Pellegrini S, et al. Bronchioloalveolar lung carcinomas: K-ras mutations are constant events in the mucinous subtype. *J Pathol.* 1996;179(3):254–259.

160. Sakuma Y, Matsukuma S, Yoshihara M, et al. Distinctive evaluation of nonmucinous and mucinous subtypes of bronchioloalveolar carcinomas in EGFR and K-ras gene-mutation analyses for Japanese lung adenocarcinomas: confirmation of the correlations with histologic subtypes and gene mutations. *Am J Clin Pathol.* 2007;128(1):100–108.

161. Tam IY, Chung LP, Suen WS, et al. Distinct epidermal growth factor receptor and KRAS mutation patterns in non-small cell lung cancer patients with different tobacco exposure and clinicopathologic features. *Clin Cancer Res.* 2006;12(5):1647–1653.

162. Marchetti A, Martella C, Felicioni L, et al. EGFR mutations in non-small-cell lung cancer: analysis of a large series of cases and development of a rapid and sensitive method for diagnostic screening with potential implications on pharmacologic treatment. *J Clin Oncol.* 2005;23(4):857–865.

163. Sonobe M, Manabe T, Wada H, Tanaka F. Mutations in the epidermal growth factor receptor gene are linked to smoking-independent, lung adenocarcinoma. *Br J Cancer.* 2005;93(3):355–363.

164. Ohtsuka T, Watanabe K, Kaji M, Naruke T, Suemasu K. A clinicopathological study of resected pulmonary nodules with focal pure ground-glass opacity. *Eur J Cardiothorac Surg.* 2006;30(1):160–163.

165. Takeuchi T, Tomida S, Yatabe Y, et al. Expression profile-defined classification of lung adenocarcinoma shows close relationship with underlying major genetic changes and clinicopathologic behaviors. *J Clin Oncol.* 2006; 24(11):1679–1688.

166. Bryant CM, Albertus DL, Kim S, et al. Clinically relevant characterization of lung adenocarcinoma subtypes based on cellular pathways: an international validation study. *PLoS ONE.* 2010;5(7):1–13.

167. Conde E, Angulo B, Tang M, et al. Molecular context of the EGFR mutations: evidence for the activation of mTOR/S6K signaling. *Clin Cancer Res.* 2006;12(3 pt 1):710–717.

168. Ohtsuka K, Ohnishi H, Furuyashiki G, et al. Clinico-pathological and biological significance of tyrosine kinase domain gene mutations and overexpression of epidermal growth factor receptor for lung adenocarcinoma. *J Thorac Oncol.* 2006;1(8):787–795.

169. Soh J, Toyooka S, Ichihara S, et al. Sequential molecular changes during multistage pathogenesis of small peripheral adenocarcinomas of the lung. *J Thorac Oncol.* 2008;3(4):340–347.

170. Yousem SA, Nikiforova M, Nikiforov Y. The histopathology of BRAF-V600E-mutated lung adenocarcinoma. *Am J Surg Pathol.* 2008;32(9):1317–1321.

171. Ninomiya H, Hiramatsu M, Inamura K, et al. Correlation between morphology and EGFR mutations in lung adenocarcinomas: significance of the micropapillary pattern and the hobnail cell type. *Lung Cancer.* 2009;63(2):235–240.

172. Hirsch FR, Varella-Garcia M, McCoy J, et al. Increased epidermal growth factor receptor gene copy number detected by fluorescence in situ hybridization associates with increased sensitivity to gefitinib in patients with bronchioloalveolar carcinoma subtypes: a Southwest Oncology Group Study. *J Clin Oncol.* 2005;23(28):6838–6845.

173. Tang X, Shigematsu H, Bekele BN, et al. EGFR tyrosine kinase domain mutations are detected in histologically normal respiratory epithelium in lung cancer patients. *Cancer Res.* 2005;65(17):7568–7572.

174. Tanaka R, Horikoshi H, Nakazato Y, et al. Magnetic resonance imaging in peripheral lung adenocarcinoma: correlation with histopathologic features. *J Thorac Imaging.* 2009;24(1):4–9.

175. Stenhouse G, Fyfe N, King G, Chapman A, Kerr KM. Thyroid transcription factor 1 in pulmonary adenocarcinoma. *J Clin Pathol.* 2004;57(4):383–387.

176. Koga T, Hashimoto S, Sugio K, et al. Clinicopathological and molecular evidence indicating the independence of bronchioloalveolar components from other subtypes of human peripheral lung adenocarcinoma. *Clin Cancer Res.* 2001;7(6):1730–1738.

177. Kim YT, Kim TY, Lee DS, et al. Molecular changes of epidermal growth factor receptor (EGFR) and KRAS and their impact on the clinical outcomes in surgically resected adenocarcinoma of the lung. *Lung Cancer.* 2008;59(1):111–118.

178. Tsuta K, Ishii G, Nitadori J, et al. Comparison of the immunophenotypes of signet-ring cell carcinoma, solid adenocarcinoma with mucin production, and mucinous bronchioloalveolar carcinoma of the lung characterized by the presence of cytoplasmic mucin. *J Pathol.* 2006;209(1):78–87.

179. Ang DC, Zakowski MF, Ladanyi M, Moreira AL, Rekhtman N. Characteristic morphology and immunoprofile of lung adenocarcinoma with KRAS mutations: propensity for solid growth pattern and correlation with TTF-1 expression. *Mod Pathol.* 2010;23(suppl 2):396A.

180. Shrestha B, Ebihara Y, Osakabe Y, Kato H. Immunohistochemical, ultrastructural and molecular study of well differentiated adenocarcinomas of the lung predominantly composed of goblet cells. *Lung Cancer.* 1998;22(2):103–117.

181. Yatabe Y, Koga T, Mitsudomi T, Takahashi T. CK20 expression, CDX2 expression, K-ras mutation, and goblet cell morphology in a subset of lung adenocarcinomas. *J Pathol.* 2004;203(2):645–652.

SCIENTIFIC REPORTS

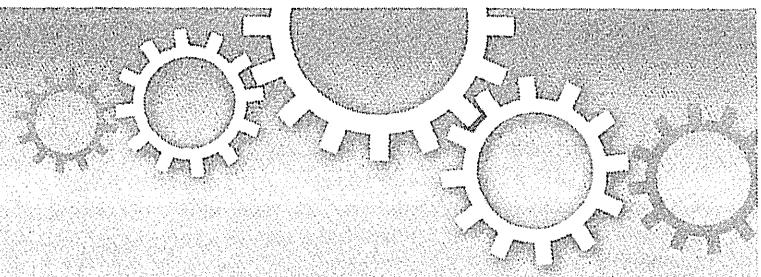

SUBJECT AREAS:
SMALL-CELL LUNG CANCER
GENE SILENCING
EPIGENOMICS
TRANSLATIONAL RESEARCH

Received
25 February 2013

Accepted
14 May 2013

Published
29 May 2013

Correspondence and requests for materials should be addressed to A.K. (kaneda@genome.rcast.u-tokyo.ac.jp)

PRC2 overexpression and PRC2-target gene repression relating to poorer prognosis in small cell lung cancer

Teruyuki Sato[1,2], Atsushi Kaneda[1,3,4], Shingo Tsuji[1], Takayuki Isagawa[1], Shogo Yamamoto[1], Takanori Fujita[1], Ryota Yamanaka[1], Yukiko Tanaka[1], Toshihiro Nukiwa[2], Victor E. Marquez[5], Yuichi Ishikawa[6], Masakazu Ichinose[2] & Hiroyuki Aburatani[1]

[1]Genome Science Division, Research Center for Advanced Science and Technology (RCAST), The University of Tokyo, Japan, [2]Department of Respiratory Medicine, Graduate School of Medicine, Tohoku University, Japan, [3]Department of Molecular Oncology, Graduate School of Medicine, Chiba University, Japan, [4]CREST, Japan Science and Technology Agency (JST), [5]Chemical Biology Laboratory, Frederick National Laboratory for Cancer Research, National Cancer Institute, USA, [6]Divison of Pathology, the Cancer Institute Hospital, Japanese Foundation for Cancer Research, Japan.

Small cell lung cancer (SCLC) is a subtype of lung cancer with poor prognosis. Expression array analysis of 23 SCLC cases and 42 normal tissues revealed that *EZH2* and other PRC2 members were highly expressed in SCLC. ChIP-seq for H3K27me3 suggested that genes with H3K27me3(+) in SCLC were extended not only to PRC2-target genes in ES cells but also to other target genes such as cellular adhesion-related genes. These H3K27me3(+) genes in SCLC were repressed significantly, and introduction of the most repressed gene *JUB* into SCLC cell line lead to growth inhibition. Shorter overall survival of clinical SCLC cases correlated to repression of *JUB* alone, or a set of four genes including H3K27me3(+) genes. Treatment with EZH2 inhibitors, DZNep and GSK126, resulted in growth repression of SCLC cell lines. High PRC2 expression was suggested to contribute to gene repression in SCLC, and may play a role in genesis of SCLC.

Lung cancer is the most leading cause of cancer-related deaths in the world, accounting for about 1.4 million deaths each year[1]. Small cell lung cancer (SCLC) is a histologic subtype of lung cancer with a distinct clinical and biological feature, and represents approximately 15% of all the lung cancer cases[2,3]. SCLC is strongly related to cigarette smoking, and approximately 90% of cases are reported to be smokers[4,5]. The prognosis is poor mainly due to early dissemination and rapid growth[6,7]. While SCLC shows high response to initial therapy, most cases relapse and become refractory to treatment. The 5-year survival is as poor as 15–25% for cases at limited stage, and <1% for cases at extensive stage[6,8,9].

Frequent mutation of *TP53* and *RB1* is reported in SCLC[10]. Sutherland *et al.* reported that cell type-restricted inactivation of *Trp53* and *Rb1* in mouse lung neuroendocrine cells and alveolar type 2 cells induced formation of lung tumors with extrapulmonary metastasis resembling SCLC[11]. Whole genome sequencing of SCLC cell line NCI-H209 revealed >20,000 somatic substitutions including 134 of those in coding exons, and rearrangement of *CHD7*[12]. Rudin *et al.* analyzed exome, transcriptome and copy number aberration of clinical SCLC samples, normal tissues, SCLC cell lines and normal cell lines, and identified 22 significantly mutated cancer-associated genes in SCLC, including *TP53* and *RB1*. Furthermore they found *SOX2* amplification and *RLF-MYCL1* fusion[13]. Peifer *et al.* also performed integrative analysis of exome/genome sequencing, transcriptome, and copy number aberrations in 29 SCLC. They reported *TP53* and *RB1* inactivation, mutations in *PTEN*, *SLIT2*, and *EPHA2*, and recurrent mutation of histone modifiers e.g. *CREBBP*, *EP300*, and *MLL*[14].

Polycomb Repressive Complexes (PRCs) are known to modify epigenetic status and repress their target genes to establish and maintain the cell fates[15,16]. EZH2 is a catalytic component of PRC2 and functions as a histone methyltransferase for H3 lysine 27 residue (H3K27), and its overexpression in cancer was reported first in prostate cancer, followed by breast cancer. EZH2 overexpression correlates to cancer progression and poorer prognosis[17,18]. On the other hand, SWI/SNF antagonizes PRCs and activates PRC target genes and contributes to cell differentiation. Mutation in proteins in SWI/SNF complex leads to loss of antagonistic function to polycomb complex protein[19]. Those mutations or high expression of EZH2 may play a role in maintenance of cell stemness and thus carcinogenesis[20]. As for lung cancer, 3-Deazaneplanocin A (DZNep), an inhibitor of PRC2, inhibits

growth of non-small cell lung cancer cells compared to non-cancerous bronchial epithelial and fibroblast cells[21]. Furthermore, immunohistochemical analysis suggested that elevated EZH2 expression is associated with non-small cell lung cancer progression and metastasis[22].

Involvement of PRC2 in SCLC, however, has not been elucidated. Here we report high expression levels of *EZH2* and other PRC2 components in SCLC. Genes with H3K27me3(+) in SCLC cell lines but H3K27me3(−) in normal small airway epithelial cell (SAEC), (i) did not overlap with PRC2-target genes in ES cells, (ii) showed lower expression levels not only in SCLC cell lines but also in clinical SCLC samples, and (iii) showed significant enrichment of GO-terms e.g. immune response, cell adhesion, and plasma membrane. While *JUB* is the most repressed gene with such GO-terms and with H3K27me3 mark in all the three SCLC cell lines, *JUB* introduction lead to growth inhibition. Shorter overall survival of clinical SCLC cases correlated to repression of *JUB* alone, or a set of four genes including PRC target genes and marker genes of classic type SCLC[23–25]. It is suggested that high expression of PRC2 contributes to gene repression in SCLC, and the gene repression may play a role in genesis of SCLC.

Results

Microarray expression analysis in SCLC and normal tissues. Gene expressions in 23 clinical SCLC samples and 42 normal tissues including the normal lung were analyzed on genome-wide scale using microarray, and average expression levels of SCLC were compared to those of normal tissues. Among 11,037 genes with Genechip score >200 in at least one sample, 71 genes showed higher expression in SCLC by >10-fold compared to normal tissues (Supplementary Table S1). The most highly expressed genes in SCLC samples included *GRP*, *INSM1* and *ASCL1*, which were reported to be highly expressed in classic type SCLC with neuroendocrine features[23–25], *TOP2A*, which encodes a DNA topoisomerase active in fast-growing tumors and is a target of chemotherapy in SCLC[26], and *EZH2*, a member of PRC2 and a methyltransferase for histone H3 lysine K27 (Fig. 1). Other PRC2 members, *SUZ12* and *EED*, were also highly expressed in SCLC compared to the normal tissues. The expression levels of PRC2 members in SCLC were also significantly higher than squamous cell carcinoma and adenocarcinoma of the lung (Supplementary Fig. S1).

Mapping of histone modification. We performed ChIP-seq for H3K27me3 mark in three SCLC cell lines and in SAEC, and obtained 9280, 9352, 15704 and 7589 peaks in Lu130, H209, DMS53, and SAEC, respectively (Fig. 2a). We then prepared ChIP samples by additionally performed ChIP experiments, and performed quantitative ChIP-PCR to validate ChIP-seq results (Fig. 2b). To confirm overlapping of H3K27me3(+) regions and PRC2-target regions, we also performed ChIP-seq for SUZ12 in a SCLC cell line Lu130. SUZ12(+) regions were well-overlapped to H3K27me3(+) regions as reported[27,28] (Supplementary Fig. S2).

Genes with and without H3K27me3 around promoter region (within ± 2kb from transcription start site) were regarded as H3K27me3(+) and H3K27me3(−) genes, respectively. When expression levels of H3K27me3(+) genes were compared to H3K27me3(−) genes within each sample, H3K27me3(+) genes showed significant repression: 0.11-fold in SAEC, 0.27-fold in Lu130, 0.08-fold in H209, and 0.11-fold in DMS53 ($P < 1 \times 10^{-20}$, *t*-test), confirming that ChIP-seq analysis for H3K27me3 was properly performed (Fig. 2c).

These H3K27me3(+) genes were compared with reported PRC2-target genes in ES cells[28]. Genes with H3K27me3 in SAEC only or genes with H3K27me3 in both SAEC and SCLC cell lines, showed significant overlap with PRC2-target genes in ES cells. Genes with H3K27me3 in SCLC cell lines but not in SAEC, however, were not significantly overlapped with PRC2-target genes in ES cells (Fig. 2d).

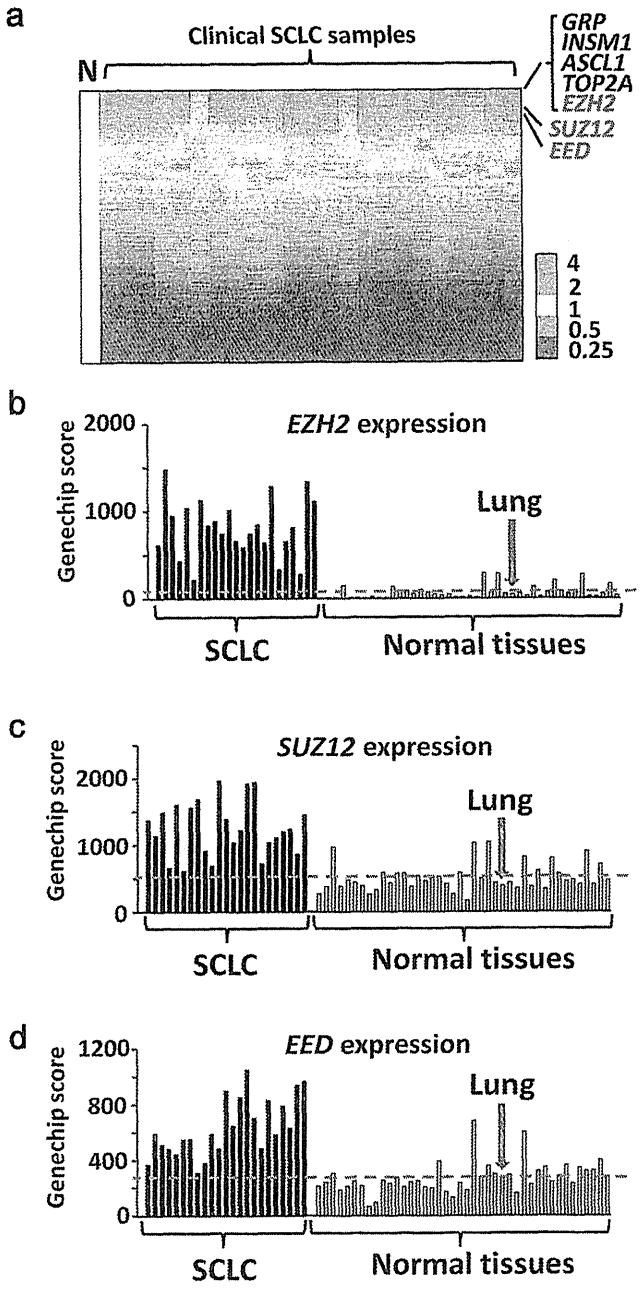

Figure 1 | Expression levels of PRC2 components in SCLC. Gene expression levels in 23 clinical SCLC samples were analyzed using expression arrays, and compared to 42 normal tissues including the lung. (a) Heatmap of gene expression in SCLC. Expression levels were shown by the ratio to the average expression level of all the normal samples (*N*), and genes were sorted by the descending order of average expression levels in SCLC samples. Ezh2 was one of the most highly expressed genes. Expression levels of *EZH2* (b) and other PRC2 members, *SUZ12* (c) and *EED* (d), in SCLC samples were significantly higher than normal samples ($P = 3 \times 10^{-10}$, 7×10^{-9}, 1×10^{-8}, respectively, *t*-test). *Red bar*, the average expression level of the normal samples. Expression levels were shown by Genechip Score.

Genes repressed with H3K27me3 in SCLC. The 8,654 genes showing H3K27me3(−) in 3 SCLC cell lines and also H3K27me3(−) in SAEC (SCLC(3-)SAEC(−) genes), showed similar

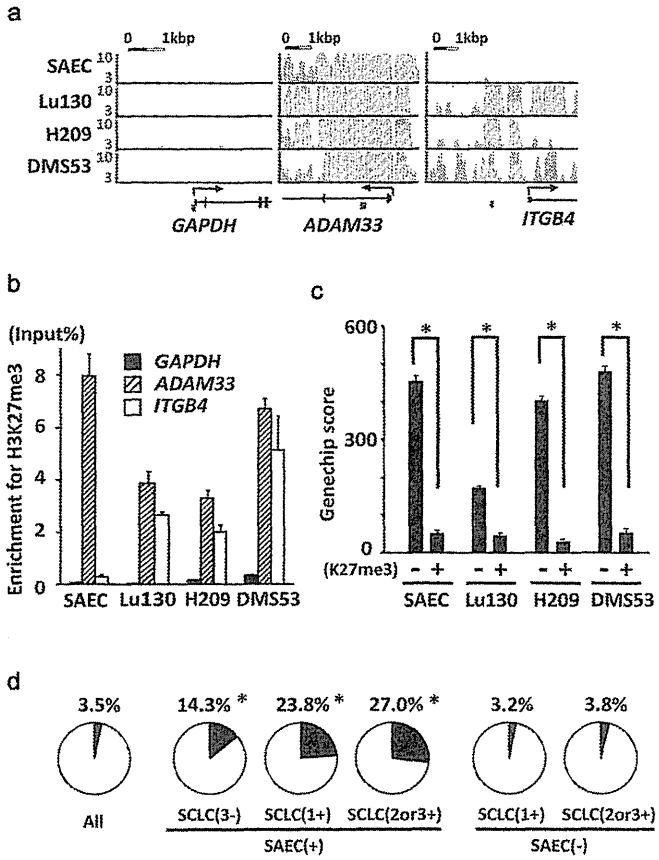

Figure 2 | Identification of genes modified with H3K27me3 in SCLC cell lines. (a) ChIP-seq of H3K27me3 in SAEC and SCLC cell lines. Genes not modified with H3K27me3 in either SAEC or SCLC cell lines (*GAPDH*), modified both in SAEC and SCLC cell lines (*ADAM33*), and not modified in SAEC but in SCLC cell lines (*ITGB4*), were representatively shown. *Brown bars*, regions for ChIP-PCR. (b) The results of ChIP-seq in *GAPDH*, *ADAM33* and *ITGB4* were validated by real-time PCR using ChIP samples that were obtained in additionally performed ChIP experiments. (c) Expression of H3K27me3(+) genes was significantly lower than H3K27me3(−) genes in each sample (*$P < 10^{-20}$, *t*-test). (d) PRC2-target genes in ES cells[28] occupied 3.5% among all the genes (*left*). Among genes with H3K27me3 in SAEC only, in SAEC and 1 SCLC cell line, and in SAEC and 2–3 SCLC cell lines (*center*), PRC2-target genes in ES cells occupied 14.3%, 23.8%, and 27.0%, respectively, indicating significant overlap (*$P < 10^{-30}$, $P < 10^{-30}$, $P < 10^{-30}$, Fisher's exact test.). Genes with H3K27me3 in 1 SCLC cell line or 2–3 SCLC cell lines but not in SAEC (*right*), however, were not significantly overlapped with PRC2-target genes in ES cells, 3.2% ($P = 0.66$) or 3.8% ($P = 0.65$), respectively.

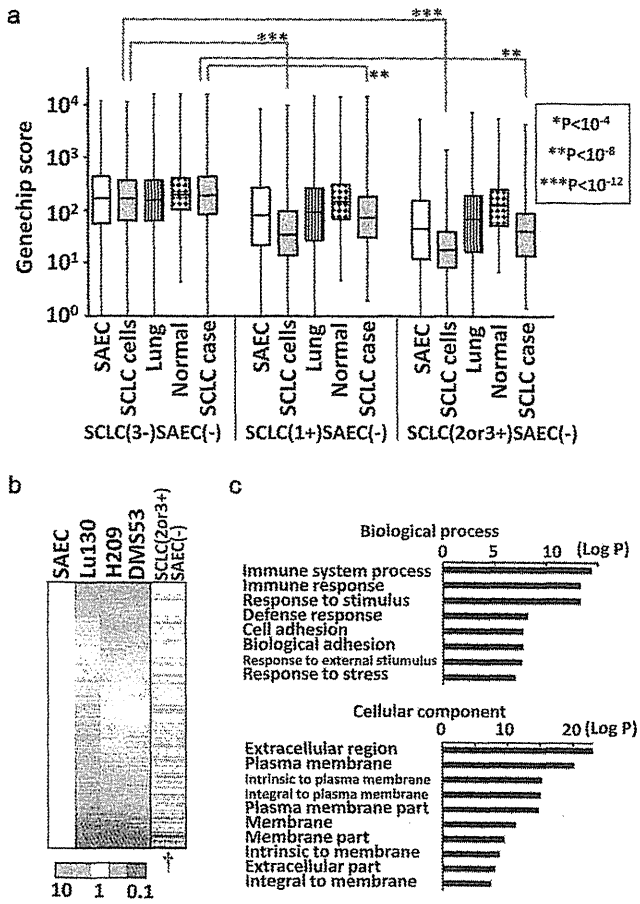

Figure 3 | Repression of genes with H3K27me3 in SCLC. (a) Gene expression in clinical samples. As for SCLC(3-)SAEC(−) genes showing H3K27me3(−) in all the three SCLC cell lines and H3K27me3(−) in SAEC (*left*), gene expression levels were similar among SAEC, SCLC cell lines, the lung, the normal other tissues, and clinical SCLC samples. As for SCLC(1+)SAEC(−) genes showing H3K27me3(+) in one SCLC cell line but H3K27me3(−) in SAEC (*middle*), expression levels were significantly lower in SCLC cell lines and clinical SCLC samples when compared between SCLC(3-)SAEC(−) and SCLC(1+)SAEC(−) categories. As for SCLC(2or3+)SAEC(−) genes showing H3K27me3(+) in two or three SCLC cell lines but H3K27me3(−) in SAEC (*right*), expression levels were even lower in SCLC cell lines and clinical SCLC samples when compared between SCLC(3-)SAEC(−) and SCLC(2or3+)SAEC(−) categories. (b) Significant repression of H3K27me3(+) genes in SCLC. Gene expression levels were shown by the ratio to those of SAEC, and all the genes were sorted by the descending order of average expression levels in SCLC cell lines. Genes in SCLC(2or3+)SAEC(−) category (*black bar* in the most right column) showed significant enrichment downward (†$P < 10^{-15}$, Kolmogorov-Smirnov test), indicating that H3K27me3 modification at promoter regions correlated to gene repression. (c) GO-terms with significant enrichment. Immune response ($P = 5.1 \times 10^{-14}$), cell adhesion ($P = 1.7 \times 10^{-8}$), extracellular region ($P = 1.3 \times 10^{-23}$), plasma membrane ($P = 8.1 \times 10^{-21}$), and terms similar to these, showed significant enrichment in SCLC(2or3+)SAEC(−) genes.

expression levels among SAEC, 3 SCLC cell lines, the normal lung, other normal tissues, and clinical SCLC cases (Fig. 3a). But the 644 genes showing H3K27me3(+) in 1 of 3 SCLC cell lines but H3K27me3(−) in SAEC (SCLC(1+)SAEC(−) genes), showed lower expression levels in SCLC cell lines as well as clinical SCLC cases compared to the SCLC(3-)SAEC(−) genes. The 343 genes showing H3K27me3(+) in 2 or 3 SCLC cell lines but H3K-27me3(−) in SAEC (SCLC(2or3+)SAEC(−) genes), showed further reduced expression levels in SCLC cell lines as well as clinical SCLC cases compared to the SCLC(3-)SAEC(−) genes. These data indicated that genes with H3K27me3(+) in SCLC cell lines were significantly repressed not only in the analyzed SCLC cell lines, but also in clinical SCLC samples (Fig. 3a).

When genes were sorted by fold expression level between SAEC and mean of 3 SCLC cell lines in descending order, the SCLC (2or3+)SAEC(−) genes were significantly enriched downward ($P < 1 \times 10^{-15}$, Kolmogorov-Smirnov test), i.e. were significantly repressed in SCLC cell lines (Fig. 3b). The 343 SCLC(2or3+) SAEC(−) genes showed significant enrichment of GO-terms e.g. immune response ($P = 5.1 \times 10^{-14}$), cell adhesion ($P = 1.7 \times 10^{-8}$) and other similar terms in Biological Process, which were different from GO-terms of PRC2-target genes in ES cells related to differentiation and development. Extracellular region ($P = 1.3 \times 10^{-23}$), plasma membrane ($P = 8.1 \times 10^{-21}$) and other similar GO-terms were enriched in Cellular Component (Fig. 3c).

Introduction of repressed genes in SCLC cell line. Genes possessing H3K27me3 mark in all the three SCLC cell lines, and relating to the four GO-terms of immune response, cell adhesion, extracellular region, or plasma membrane, were sorted by fold expression level between SAEC and mean of 3 SCLC cell lines in descending order (Fig. 4a). The most repressed genes were *JUB* and *PTRF*, which showed decreased expression to 0.01-fold in SCLC cell lines compared to SAEC, and H3K27me3 mark specifically in SCLC cell lines (Fig. 4b). These two genes were introduced in an SCLC cell line DMS53 using lentiviral system, and the protein expressions were confirmed by western blotting (Fig. 5a and Supplementary Fig. S3). JUB was distributed to the cellular membrane, while PTRF was localized in the cytoplasm (Fig. 5b). Introduction of *JUB* inhibited cellular growth, whereas introduction of *PTRF* did not affect cellular growth (Fig. 5c), suggesting that the most repressed gene related to cell adhesion, *JUB*, might function as a growth-suppressor in SCLC cells and its repression by PRC2 might contribute to genesis of SCLC.

JUB repression correlated to shorter survival. Since gene repression by PRC2 was suggested to contribute to genesis of SCLC, we wanted to analyze whether the repression correlated to poorer prognosis of clinical SCLC or not. We therefore examined the dependency of overall survival time on *JUB* and other highly repressed PRC-target genes (*PTRF, DMKN, AXL, EPHB4*) (Fig. 4a) as well as highly expressed PRC2 complex genes (*EZH2, SUZ12, EED*) and also highly expressed classic type marker genes (*GRP, INSM1, ASCL1*) (Fig. 1a), using the Cox proportional-hazards regression. Repression of *JUB* or *EPHB4* showed strong correlation to shorter survival ($P = 0.002$ or $P = 0.007$, respectively), while high expression of classic type marker, *GRP*, also correlated to shorter survival ($P = 0.02$) (Fig. 6a). The most relevant predictor variables were analyzed by the AIC based criteria, the stepAIC function of R software, and a set of four genes, *JUB, EPHB4, GRP* and *ASCL1*, was selected as the most relevant one ($P = 0.0001$) among all the possible combination of one through 11 genes. The K-means sample clustering with the four genes using Orange software[29] showed that the optimal cluster size was two, and the two groups of samples were shown by the multi dimensional scaling plot (Fig. 6b). The one group (namely Group-L) could be simply characterized with low *JUB* and high *GRP* expression, and the other one (namely Group-H), opposite (Fig. 6c). To analyze whether the classification into the two clusters reflect distinct prognosis, Kaplan-Meyer survival analysis was also performed. Group-L showed shorter overall survival than Group-H ($P = 0.02$, log-rank test) (Fig. 6d).

To confirm the robustness of the set of four genes to classify SCLC, we analyzed reported RNA-seq data of SCLC[14]. The optimal cluster size was again two, revealed by the K-means sample clustering with the four genes using Orange[29], and the two groups of samples were shown by the multi dimensional scaling plot (Supplementary Fig. S4a). Again, the Group-L could be simply characterized with low *JUB* and high *GRP* expressions, and the Group-H, opposite (Supplementary Fig. S4b).

Treatment of SCLC cell lines with EZH2 inhibitors. To get insight into clinical application of EZH2 inhibitors on SCLC, we next analyzed effect of an EZH2 inhibitor, DZNep[30,31], on the three SCLC cell lines *in vitro*. When SCLC cell lines were treated with 5 μM DZNep for 5–6 days, western blot analysis showed decrease of EZH2 protein level (Fig. 7a and Supplementary Fig. S5), which is consistent with the previous report[32]. WST-8 assay showed repression of cellular growth in the three SCLC cell lines,

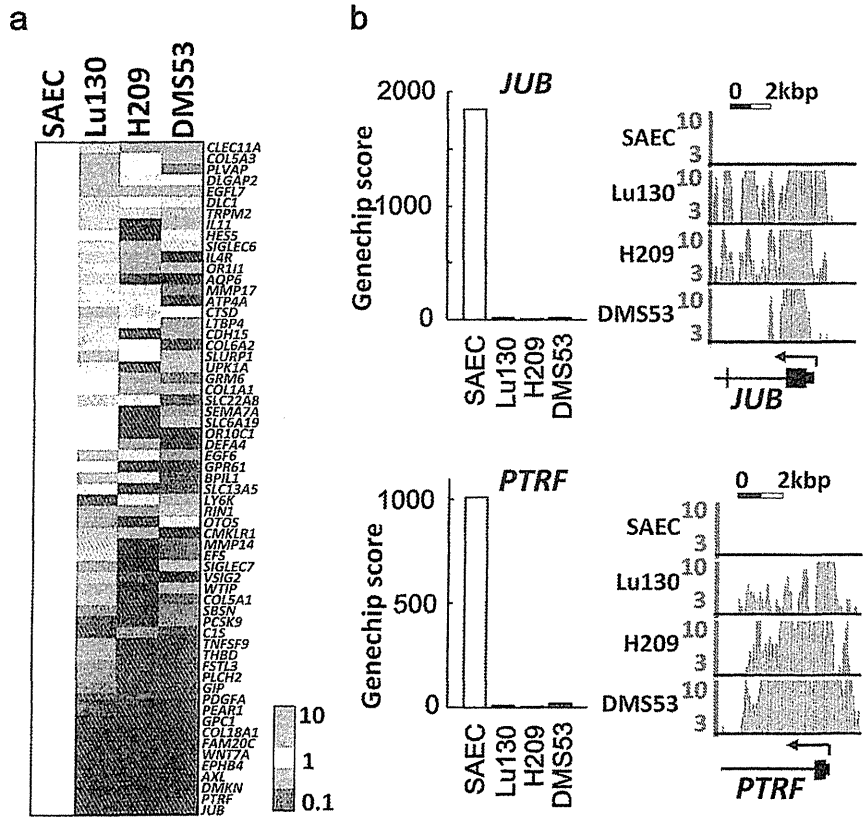

Figure 4 | Genes most repressed with H3K27me3 in SCLC. (a) Genes that showed H3K27me3 in all the three SCLC cell lines, and that were included in the four GO-terms of Immune response, cell adhesion, extracellular region, and plasma membrane. They were sorted by the descending order of average expression levels in SCLC cell lines, and the most repressed genes were *JUB* and *PTRF*. (b) SCLC cell lines showed low expression levels and H3K27me3 modifications of *JUB* and *PTRF*.

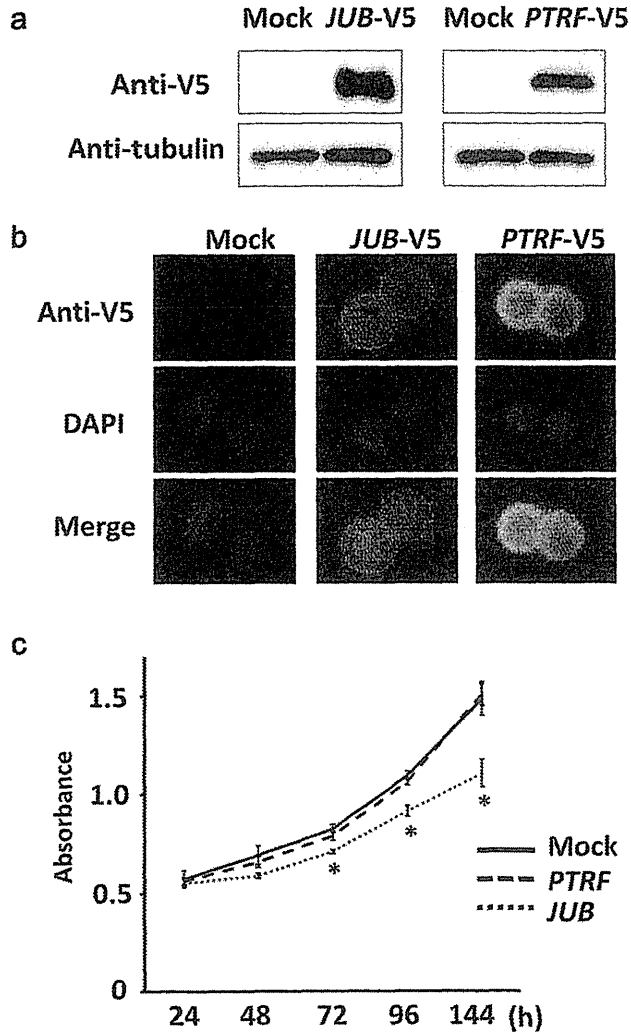

Figure 5 | **Introduction of *JUB* and *PTRF* in SCLC cell line.** *JUB* or *PTRF* cDNA with V5-tag was introduced in SCLC cell line DMS53 by lentivirus infection. (a) Expression was confirmed by western blotting. Blots were cropped in the figure, but the gels were run under the same experimental conditions, and full-length blots are presented in Supplementary Fig. S3. (b) JUB and PTRF expression by immunofluorescence. Introduced JUB was mainly observed at plasma membrane, and introduced PTRF was mainly observed in the cytoplasm. (c) Growth curve analyzed by WST-8 assay. PTRF-introduced cells showed similar growth to mock cells infected with empty lentivirus, whereas JUB-introduced cells showed suppressed growth significantly (*P < 0.05, *t*-test). *Bars*, standard deviation in triplicated analysis.

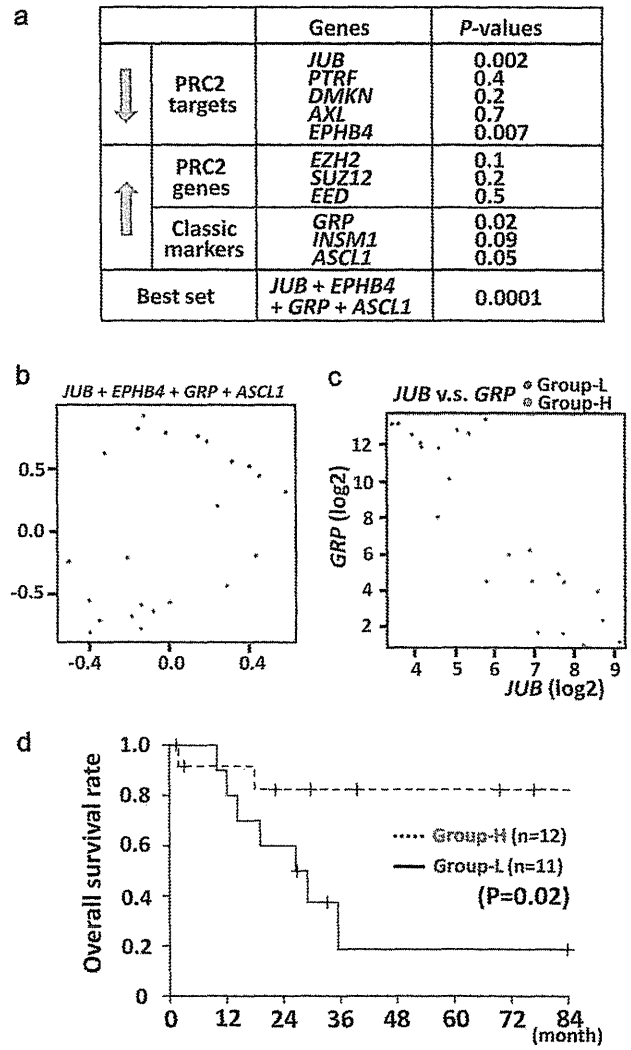

Figure 6 | **Lower expression of *JUB* and poorer prognosis.** (a) For five of repressed PRC-target genes (*downward arrow*) and six of highly expressed genes (*upward arrow*), the dependency of overall survival time of SCLC cases on each gene was analyzed using the Cox proportional-hazards regression, e.g. P = 0.002 for *JUB*. Among all the possible combination of one through 11 genes, the most relevant predictor variables were the set of the four genes, *JUB*, *EPHB4*, *GRP* and *ASCL1* (*bottom*, P = 0.0001). (b) The K-means sample clustering using the four genes showed that the optimal cluster size of SCLC cases was two, and the two groups of samples (*blue* and *red* spots) were shown by the multi dimensional scaling plot. (c) The one group (*blue*) could be simply characterized with low *JUB* and high *GRP* expression, and thus called Group-L. The other one (*red*) showed high *JUB* and low *GRP* expression, and thus called Group-H. (d) Group-L showed shorter recurrence-free survival than Group-H (P = 0.02, log-rank test).

suggesting that EZH2 inhibitors might be effective for therapy on SCLC.

SCLC cell lines were then treated with a selective EZH2 inhibitor, GSK126, at different doses of 0.5, 2, and 8 μM (Fig. 7b). All the three cell lines showed substantial inhibition of cellular growth at high dose (8 μM). Although DMS53 was not sensitive to lower doses (0.5 μM and 2 μM), growth inhibition was observed in part at lower doses in Lu130 and H209.

Discussion

We here report high expression levels of EZH2 and other PRC2 components in SCLC. Genes targeted by PRC2 in SCLC cell lines were shown to be repressed in SCLC cell lines and clinical SCLC samples. While *JUB* is the most repressed gene with H3K27me3 mark in all the three SCLC cell lines, *JUB* introduction lead to growth inhibition of SCLC cells. Shorter overall survival of clinical SCLC cases significantly correlated to lower expression of *JUB* alone (P = 0.002), or a set of PRC2 target genes (*JUB*, *EPHB4*) and classic type marker genes (*GRP*, *ASCL1*) (P = 0.0001). Treatment of three SCLC cell lines with EZH2 inhibitors, DZNep and GSK126, induced growth inhibition. These data suggested that high expression of PRC2 contributed to gene repression in SCLC, and the repression may play a role in worse prognosis of SCLC.

PRC2 complex has a histone methyltransferase activity and represses gene expression by methylation of H3K27 residue. PRC2-target genes in ES cells[28] show enrichment of genes related to development and differentiation, and repression of those genes in ES cells or adult tissue stem cells plays a role in maintenance of

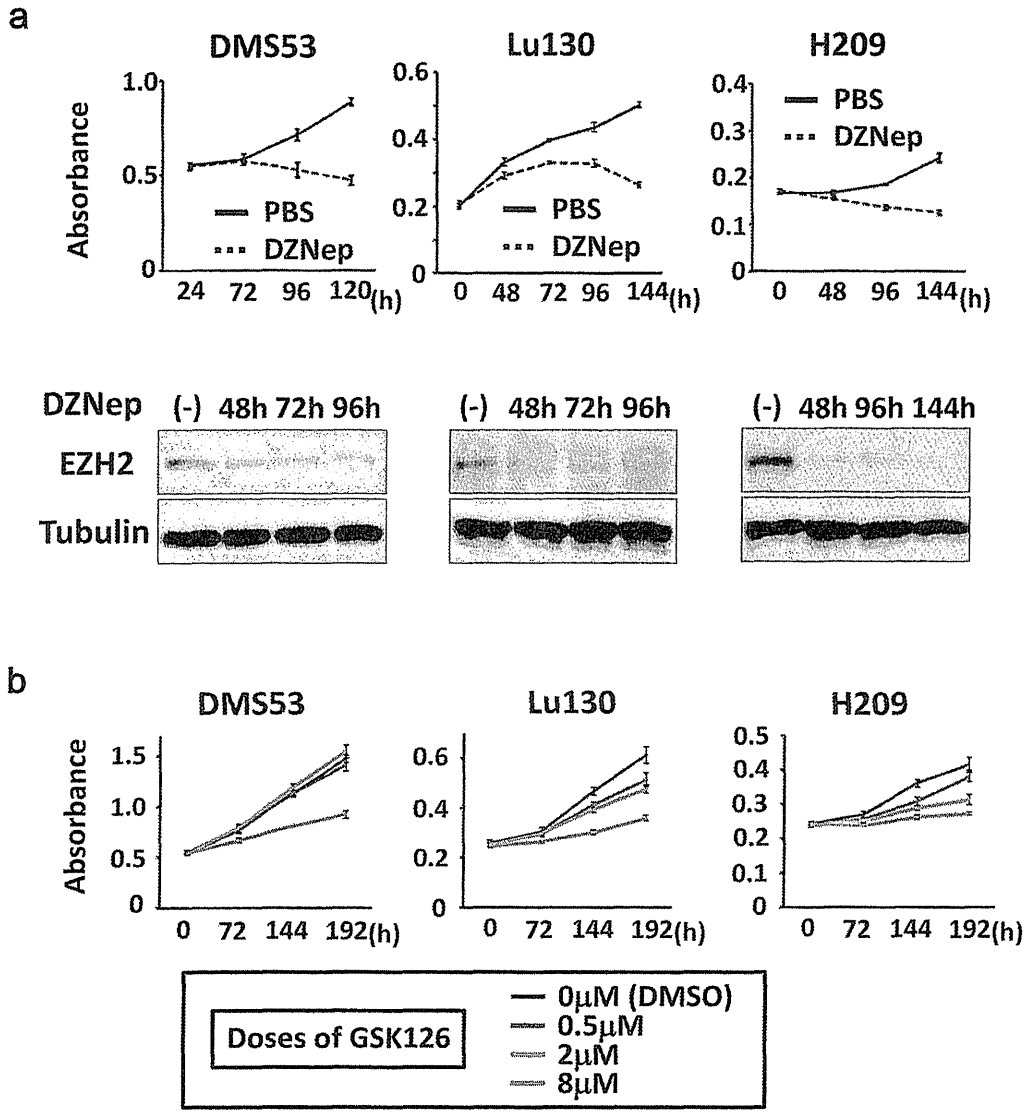

Figure 7 | Growth inhibition of SCLC cell lines by treatment with EZH2 inhibitors. (a) SCLC cell lines, Lu130, H209, and DMS53, were treated with 5 μM DZNep, and growth curve was analyzed by WST-8 assay. Inhibition of cellular growth by DZNep treatment was observed in all the three cell lines, compared to vehicle (PBS) treatment. Protein levels of EZH2 were confirmed to be decreased by DZNep treatment, by western blot analysis. Blots were cropped in the figure, but the gels were run under the same conditions, except that 7% gel was used for EZH2 and 12% gel was used for α-tubulin in analyses of Lu130 and H209. Full-length blots are presented in Supplementary Fig. S5. (b) SCLC cell lines were treated with 0.5, 2, and 8 μM GSK126, and growth curve was analyzed by WST-8 assay. Inhibition of cellular growth by GSK126 treatment was observed at 8 μM in all the three cell lines, while Lu130 and H209 were more sensitive to GSK126, even at lower doses.

stemness[33]. In this study, genes with H3K27me3 in SAEC only and genes with H3K27me3 both in SAEC and SCLC cells were significantly overlapped with PRC2-target genes in ES cells, and showed enrichment of GO-terms such as development and differentiation, similar to PRC2-target genes in ES cells. Genes with H3K27me3 in SCLC cells but not in SAEC, however, were not overlapped with PRC2-target genes in ES cells (Fig. 2d). It might be suggested that H3K27me3 marks in SCLC might be extended to not only PRC2-target genes in ES cells but also other target genes such as cellular adhesion-related genes, due to highly expressed PRC2 components.

It was reported that high expression levels of EZH2 in prostate cancer and breast cancer correlated to metastasis and invasion, and thus poorer prognosis[17,18]. Inhibition of PRC2 by DZNep treatment resulted in growth inhibition of cancer cell lines with high expression of EZH2, compared to normal cell lines. *DAB21P* and *p21*^{CDKN1A} were reported to be PRC2 target genes and play a role in these cancers[34–36]. In SCLC, high expression of EZH2 may extend PRC2-target genes including *JUB*, and its repression in SCLC correlated to poorer prognosis. DZNep treatment of SCLC cell lines also resulted in growth inhibition, while DZNep is known as PRC2 inhibitor[30,31].

Recently, EZH2-specific inhibitors were reported to be developed and effective to diffuse large B-cell lymphoma cell lines[37,38]. Although GSK126 induced loss of H3K27me3 independent of EZH2 mutation status, six of seven lymphoma cell lines sensitive to GSK126 treatment were *EZH2*-mutation(+), while only two of 11 lymphoma cell lines less sensitive to GSK126 were *EZH2*-mutation(+). It was suggested that lymphoma cell lines with mutant EZH2 tend to be dependent on EZH2 activity on cell growth[37]. In our study, two of three SCLC cell lines showed growth inhibition in part at lower doses of GSK126. It might be suggested that elevated EZH2 in SCLC could induce the dependence of cellular growth on EZH2 activity, like the reported seven sensitive lymphoma cell lines (six EZH2-mutation(+) and one EZH2-mutation(−) cells), but that co-occurring alterations could perhaps weaken the dependency on EZH2 in some

SCLC cells. PRC2-target medicine may become an important therapeutic strategy against cancer including SCLC, and application of EZH2-specific inhibitors should be further analyzed for SCLC.

While introduction of *JUB* showed growth suppression, introduction of *PTRF* had no effect. PTRF as well as CAV1 is known as structural component of caveolae, 50–100 nm flask-shaped invaginations of plasma membrane involved in numerous signal transductions[39]. Whereas CAV1 was reported as a tumor suppressor[40,41] and PTRF was required for premature senescence induction through interaction with CAV1[42], CAV1 was also strongly repressed in the three SCLC cell lines and clinical SCLC samples (Supplementary Fig. 6). Introduction of *PTRF* together with *CAV1* might be necessary to rule out tumor-suppressive function of *PTRF* in SCLC. Beside *JUB* and *PTRF*, genes with H3K27me3 in SCLC but not in SAEC included *EPHB4*, *WNT7A*, *COL18A1*, and *THBD* (Fig. 4). *EPHB4* was reported to be a tumor suppressor gene silenced by DNA hypermethylation in acute lymphoblastic leukemia, and transduction of *EPHB4* resulted in down-regulation of phosphorylated Akt[43]. *WNT7A* was reported to be decreased in non-small cell lung cancer (NSCLC), and its transfection into NSCLC cell lines reversed malignant phenotype[44]. COL18A1 is cleaved to be Endostatin, an endogenous inhibitor of angiogenesis, and systemic administration of recombinant Endostatin inhibited growth of transplanted cancers[45]. *THBD* was reported to be a tumor suppressor gene silenced by DNA hypermethylation in cancers[46,47], and its suppression correlated to tumor invasion and poor prognosis[48,49]. Repression of these genes with H3K27me3 modification may also contribute to genesis of SCLC.

A cell adhesion-related protein JUB harbors LIM domain and is recruited to cadherin-dependent cell-cell adhesive complexes to form stable cell-cell junction[50]. JUB was also reported to bind to PRMT5 and repress SNAIL target genes in the nucleus[51], and accumulation of JUB in the nucleus of P19 embryonal cells resulted in growth inhibition and spontaneous endodermal differentiation[52]. In this study, introduction of *JUB* in an SCLC cell DMS53 resulted in growth repression, but the protein was distributed mainly to the cellular membrane, not in the nucleus. It is yet to be elucidated whether the protein distributed to cell-cell adhesive complexes functions as growth suppressor.

Classic type of SCLC with neuroendocrine feature is characterized with expression of GRP as well as L-dopa-decarboxylase, neuron specific enolase, and creatine kinase-BB isoenzyme[53]. ASCL1 is essential for development of neuroendocrine cells and also highly expressed in classic SCLC, and knock-down of ASCL1 inhibited colony formation in soft agar and induced apoptosis in SCLC[54,55]. Whereas *JUB* repression alone significantly correlated to shorter survival ($P = 0.002$), SCLC was classified into two groups with distinct prognosis using a set of PRC2 target genes (*JUB*, *EPHB4*) and classic type marker genes (*GRP*, *ASCL1*), and the group with poorer outcome could be simply characterized with low expression of *JUB* and high expression of *GRP* (Fig. 6c). Further study is necessary whether these expressions are independent phenomena or features of classic type SCLC include gene repression with H3K27me3.

In summary, PRC2 components were highly expressed in SCLC and contributed to gene repression, and the repression may play a role in genesis of SCLC.

Methods

Clinical samples and cell lines. Primary SCLC samples were obtained from patients undergoing pulmonary resection at Department of Surgery, Cancer Institute Hospital, with written informed consents. These samples were immediately frozen with liquid nitrogen and stored at −80°C. The frozen materials were microscopically examined by two independent pathologists, and were dissected to enrich cancer cells when necessary. Three SCLC cell lines with variable characteristics were prepared: a monolayer cell line DMS53 with wild type RB and missense mutation of p53, a floating cell line Lu130 with wild type RB and missense mutation of p53, and another floating cell line H209 with missense mutation of RB and splice site mutation of p53 (Supplementary Table S2). H209 and DMS53 were purchased from ATCC (Manassas, VA), and Lu130 was from Riken BioResource Center Cell Bank (Tsukuba, Japan). SAEC was obtained from Lonza (Basel, Switzerland). Lu130 and H209 were cultured in RPMI1640 containing penicillin and streptomycin, supplemented with 10% fetal bovine serum at 37°C in 5% CO_2. DMS53 was cultured in Dulbecco's modified Eagle's medium (DMEM) containing penicillin and streptomycin, supplemented with 10% fetal bovine serum at 37°C in 5% CO_2. SAEC was cultured according to supplier's instruction using SAGM BulletKit and Reagent Pack (Lonza). This study was certified by Ethics Committee in The University of Tokyo and in the Cancer Institute.

RNA samples. Total RNA of 23 SCLC samples, three SCLC cell lines and SAEC was extracted using Trizol (Invitrogen). RNA samples of normal tissues to include variety of organs e.g. central nervous, respiratory, gastrointestinal, endocrine, immunological, skeletal, reproductive, urinary and circulatory systems, were purchased as follows: whole brain, cerebellum, adrenal gland, salivary gland, trachea, bone marrow, testis from Clontech (Mountain View, CA); cereberal cortex, pons, hippocampus, diencephalon, thalamus, tongue, esophagus, gallbladder, tonsil, artery, vein, adipose, lymph node, seminal vesicle from Biochain (Newark, CA); thymus, ovary, skeletal muscle, heart, small intestine, colon, pancreas, kidney, bladder, spleen, prostate from Ambion (Carlsbad, CA); skin, thyroid, breast, and uterus from Stratagene (Santa Clara, CA). The quality of RNA was controlled using Bioanalyzer 2100 (Agilent Technology, CA) and high quality RNA with RNA intensity number (RIN) ≥7.0 was used for array analysis.

Expression array analysis. For genome-wide transcription analysis, Affymetrix GeneChip Human Genome U133 plus 2.0 oligonucleotide arrays (Fremont, CA) was used. Data were collected and analyzed by GeneChip Scanner 3000 (Affymetrix). The GeneChip data were analyzed using the Affymetrix GeneChip Operating Software v1.3 by MAS5 algorithms, to obtain signal value (Genechip score) for each probeset. For global normalization, the average signal in an array was made equal to 100. Expression array data is available at GEO datasets (GSE43346). Expression levels of squamous cell carcinoma and adenocarcinoma of the lung analyzed also using U133 plus 2.0 oligonucleotide arrays were collected from GEO datasets (GSE2199), and global normalization was done by the same manner.

Gene ontology analysis. Gene annotation enrichment analysis was done for Gene Ontology (biological process and cellular component) using the Functional Annotation tool at DAVID Bioinformatics Resources 6.7 (http://david.abcc.ncifcrf.gov/).

Chromatin immunoprecipitation (ChIP). Cells were cross-linked with 1% formaldehyde for 10 min at room temperature and were prepared for ChIP. ChIP using H3K27me3 (07-142, Upstate, rabbit polyclonal), or Suz12 (D39F6, Cell Signaling, rabbit monoclonal) antibody was performed as we previously reported[56]. Briefly, cells were crosslinked with 1% formalin for 10 min, and crosslinked cell lysates underwent fragmentation by sonication and incubated with antibodies bound to protein A-sepharose beads (50% slurry) overnight at 4°C. The beads were washed several times and eluted with elution buffer (1% SDS, 0.1 M NaHCO3). The eluates were treated with 1.5 μg of pronase 2 hr at 42°C then incubated at 65°C over night to reverse the crosslinks. The ChIP'ed DNA was purified by phenol/chroloform treatment and precipitated with LiCl and 70% ethanol.

ChIP-sequencing (Chip-seq). Sample preparation for ChIP-seq was performed according to the manufacturer's instructions (Illumina), and sequencing was performed using Illumina Genome Analyzer IIx as we previously reported[56]. Briefly, size fractionated DNA was extracted and a single adenosine was added using Klenow exo- (3′ and 5′ exo minus; Illumina). Illumina adaptors were then added and DNA was subjected to 20 cycles of PCR according to manufacturer's instructions. We then purified DNA and performed cluster generation and 36 cycles of sequencing on the Illumina cluster station and 1G Analyzer following the manufacturer's instructions. 36-bp single end reads were mapped to the NCBI Build #36 (UCSC hg18) reference human genome, using the Illumina pipeline software version 1.4. The numbers of uniquely mapped reads for SAEC, Lu130, H209 and DMS53 were 19,527,119 (SAEC), 7,543,376 (Lu130), 18,418,930 (H209) and 21,354,066 (DMS53) for H3K27me3, and 20,025,034 (Lu130) for Suz12. Distribution of immunoprecipitated DNA fragments was analyzed using Model-based Analysis for Chip-Seq (MACS)[57], with a window of 600 bp. Regions with $p < 10^{-30}$ and $p < 10^{-10}$ were regarded as H3K27me3(+) and SUZ12(+) regions, respectively. ChIP-seq data is available at GEO datasets (GSE43346).

Quantitative real-time ChIP-PCR. ChIP samples were amplified by real-time PCR using SYBR Green and iCycler Thermal Cycler (Bio-Rad Laboratories) and quantified by drawing the standard curve using 20, 2, 0.2, and 0.02 ng/μL sonicated genomic DNA of SAEC. The quantity of ChIP'ed DNA was shown as a ratio to Input DNA (Input %). The PCR primers and conditions are shown in Supplementary Table S3.

Lentiviral vectors. To introduce *JUB* and *PTRF* in SCLC cell, we constructed lentiviral vectors for *JUB* and *PTRF* by cloning full-length cDNAs by reverse-transcription PCR products from SAEC, into a CMV promoter driven expression vector pLentiV5 (Invitrogen, Carlsbad, CA) that contains puromycin resistance gene, and check the sequences. Lentivirus was prepared by transfection of pLentiV5 vector

together with pMD2 and psPAX2 vectors in 293T cells. DMS53 was infected with the prepared viruses, and selected using puromycin at 2 ug/mL for two days.

Immunoblot analysis. Aliquots of protein were subjected to SDS/PAGE followed by immunoblot analysis using antibodies against EZH2 (#39103, Active Motif), V5 (R960-25, Invitrogen), and α-Tubulin (DM1A, Sigma) as primary antibodies, and against rabbit IgG (sc-2004, Santa Cruz, 1 : 5,000 dilution) and mouse IgG (sc-2005, Santa Cruz) as secondary antibodies. The antibodies used were well characterized previously by us and others[56]. Proteins were transferred to nitrocellulose and the resulting immunoblots were visualized using Amersham ECL Plus (GE Healthcare) and LAS-3000 (Fujifilm, Japan), and processed using MultiGauge software (Fujifilm).

Cellular immunofluorescence. Cells were washed with PBS three times and fixed with 4% paraformaldehyde for 5 min. After washed with PBS three times, cells were permeabilized with 0.2% Triton X-100 in PBS for 10 min. Introduced proteins were detected using antibodies against V5 (R960-25, Invitrogen) as primary antibody, and green-fluorescent Alexa Fluor 488 dye-labeled anti-mouse antibody (A11029, Invitrogen) as secondary antibody. Photographs were taken with Biozero BZ-8100 (KEYENCE, Osaka, Japan).

Growth curve. *JUB*- and *PTRF*-introduced DMS53 cells were seeded at density of 1×10^3 cells/well in 96-well plate, and cellular growth was analyzed using WST-8 kit (Doijndo, Japan) at 12, 36, 60, and 84 h. Cellular growth of Lu130, H209, and DMS53 with treatment by DZNep or GSK126 (Active Biochem, NJ) was also analyzed using WST-8 kit. DZNep was dissolved in PBS at 5 mM, and cells were cultured at the final concentration of 5 μM. GSK126 was dissolved in DMSO at 10 mM, and cells were cultured at 0.5, 2, and 8 μM.

Statistical analysis. Statistical analyses were performed using *t*-test and Fisher's exact test. K-means sample clustering was performed by Orange[29] (http://orange.biolab.si/citation/). Kaplan-Meier survival analysis was performed by JMP 7 (http://www.jmp.com/) and P-value was calculated by log-rank test. Survival analysis by Cox proportional-hazards regression was performed by R software (http://www.R-project.org/). In overall survival analysis, the end of follow up period was 84 months from the primary surgery and the mean follow up time of the cases was 64 months. Death as a result of SCLC was the primary end point and deaths by other causes were censored.

1. Ferlay, J. *et al.* Estimates of worldwide burden of cancer in 2008: GLOBOCAN 2008. *Int J Cancer* **127** (12), 2893–2917 (2011).
2. Read, W. L., Page, N. C., Tierney, R. M., Piccirillo, J. F. & Govindan, R. The epidemiology of bronchioloalveolar carcinoma over the past two decades: analysis of the SEER database. *Lung Cancer* **45** (2), 137–142 (2004).
3. Devesa, S. S., Bray, F., Vizcaino, A. P. & Parkin, D. M. International lung cancer trends by histologic type: male:female differences diminishing and adenocarcinoma rates rising. *Int J Cancer* **117** (2), 294–299 (2005).
4. Brownson, R. C., Chang, J. C. & Davis, J. R. Gender and histologic type variations in smoking-related risk of lung cancer. *Epidemiology* **3** (1), 61–64 (1992).
5. Otterson, G., Lin, A. & Kay, F. Genetic etiology of lung cancer. *Oncology (Williston Park)* **6** (9), 97–104, 107; discussion **108**, 111–102 (1992).
6. Sher, T., Dy, G. K. & Adjei, A. A. Small cell lung cancer. *Mayo Clin Proc* **83** (3), 355–367 (2008).
7. Gustafsson, B. I., Kidd, M., Chan, A., Malfertheiner, M. V. & Modlin, I. M. Bronchopulmonary neuroendocrine tumors. *Cancer* **113** (1), 5–21 (2008).
8. Albain, K. S., Crowley, J. J. & Livingston, R. B. Long-term survival and toxicity in small cell lung cancer. Expanded Southwest Oncology Group experience. *Chest* **99** (6), 1425–1432 (1991).
9. Lassen, U. *et al.* Long-term survival in small-cell lung cancer: posttreatment characteristics in patients surviving 5 to 18+ years--an analysis of 1,714 consecutive patients. *J Clin Oncol* **13** (5), 1215–1220 (1995).
10. Sekido, Y., Fong, K. M. & Minna, J. D. Molecular genetics of lung cancer. *Annu Rev Med* **54**, 73–87 (2003).
11. Sutherland, K. D. *et al.* Cell of origin of small cell lung cancer: inactivation of Trp53 and Rb1 in distinct cell types of adult mouse lung. *Cancer Cell* **19** (6), 754–764 (2011).
12. Pleasance, E. D. *et al.* A small-cell lung cancer genome with complex signatures of tobacco exposure. *Nature* **463** (7278), 184–190 (2010).
13. Rudin, C. M. *et al.* Comprehensive genomic analysis identifies SOX2 as a frequently amplified gene in small-cell lung cancer. *Nat Genet* **44** (10), 1111–1116 (2012).
14. Peifer, M. *et al.* Integrative genome analyses identify key somatic driver mutations of small-cell lung cancer. *Nat Genet* **44** (10), 1104–1110 (2012).
15. Bracken, A. P. & Helin, K. Polycomb group proteins: navigators of lineage pathways led astray in cancer. *Nat Rev Cancer* **9** (11), 773–784 (2009).
16. Margueron, R. & Reinberg, D. The Polycomb complex PRC2 and its mark in life. *Nature* **469** (7330), 343–349 (2011).
17. Varambally, S. *et al.* The polycomb group protein EZH2 is involved in progression of prostate cancer. *Nature* **419** (6907), 624–629 (2002).
18. Kleer, C. G. *et al.* EZH2 is a marker of aggressive breast cancer and promotes neoplastic transformation of breast epithelial cells. *Proc Natl Acad Sci U S A* **100** (20), 11606–11611 (2003).
19. Mills, A. A. Throwing the cancer switch: reciprocal roles of polycomb and trithorax proteins. *Nat Rev Cancer* **10** (10), 669–682 (2010).
20. Wilson, B. G. *et al.* Epigenetic antagonism between polycomb and SWI/SNF complexes during oncogenic transformation. *Cancer Cell* **18** (4), 316–328 (2010).
21. Kikuchi, J. *et al.* Epigenetic therapy with 3-deazaneplanocin A, an inhibitor of the histone methyltransferase EZH2, inhibits growth of non-small cell lung cancer cells. *Lung Cancer* **78** (2), 138–143 (2012).
22. Huqun *et al.* Enhancer of zeste homolog 2 is a novel prognostic biomarker in nonsmall cell lung cancer. *Cancer* **118** (6), 1599–1606 (2012).
23. Miyake, Y., Kodama, T. & Yamaguchi, K. Pro-gastrin-releasing peptide(31–98) is a specific tumor marker in patients with small cell lung carcinoma. *Cancer Res* **54** (8), 2136–2140 (1994).
24. Bhattacharjee, A. *et al.* Classification of human lung carcinomas by mRNA expression profiling reveals distinct adenocarcinoma subclasses. *Proc Natl Acad Sci U S A* **98** (24), 13790–13795 (2001).
25. Garber, M. E. *et al.* Diversity of gene expression in adenocarcinoma of the lung. *Proc Natl Acad Sci U S A* **98** (24), 13784–13789 (2001).
26. Chhatriwala, H., Jafri, N. & Salgia, R. A review of topoisomerase inhibition in lung cancer. *Cancer Biol Ther* **5** (12), 1600–1607 (2006).
27. Kirmizis, A. *et al.* Silencing of human polycomb target genes is associated with methylation of histone H3 Lys 27. *Genes Dev* **18** (13), 1592–1605 (2004).
28. Lee, T. I. *et al.* Control of developmental regulators by Polycomb in human embryonic stem cells. *Cell* **125** (2), 301–313 (2006).
29. Curk, T. *et al.* Microarray data mining with visual programming. *Bioinformatics* **21** (3), 396–398 (2005).
30. Tan, J. *et al.* Pharmacologic disruption of Polycomb-repressive complex 2-mediated gene repression selectively induces apoptosis in cancer cells. *Genes Dev* **21** (9), 1050–1063 (2007).
31. Chase, A. & Cross, N. C. Aberrations of EZH2 in cancer. *Clin Cancer Res* **17** (9), 2613–2618 (2011).
32. Zoabi, M., Sadeh, R., de Bie, P., Marquez, V. E. & Ciechanover, A. PRAJA1 is a ubiquitin ligase for the polycomb repressive complex 2 proteins. *Biochem Biophys Res Commun* **408** (3), 393–398 (2011).
33. Juan, A. H. *et al.* Polycomb EZH2 controls self-renewal and safeguards the transcriptional identity of skeletal muscle stem cells. *Genes Dev* **25** (8), 789–794 (2011).
34. Chen, H., Tu, S. W. & Hsieh, J. T. Down-regulation of human DAB2IP gene expression mediated by polycomb Ezh2 complex and histone deacetylase in prostate cancer. *J Biol Chem* **280** (23), 22437–22444 (2005).
35. Min, J. *et al.* An oncogene-tumor suppressor cascade drives metastatic prostate cancer by coordinately activating Ras and nuclear factor-kappaB. *Nat Med* **16** (3), 286–294 (2010).
36. Fan, T. *et al.* EZH2-dependent suppression of a cellular senescence phenotype in melanoma cells by inhibition of p21/CDKN1A expression. *Mol Cancer Res* **9** (4), 418–429 (2011).
37. McCabe, M. T. *et al.* EZH2 inhibition as a therapeutic strategy for lymphoma with EZH2-activating mutations. *Nature* **492** (7427), 108–112 (2012).
38. Knutson, S. K. *et al.* A selective inhibitor of EZH2 blocks H3K27 methylation and kills mutant lymphoma cells. *Nat Chem Biol* **8** (11), 890–896 (2012).
39. Hill, M. M. *et al.* PTRF-Cavin, a conserved cytoplasmic protein required for caveola formation and function. *Cell* **132** (1), 113–124 (2008).
40. Capozza, F. *et al.* Absence of caveolin-1 sensitizes mouse skin to carcinogen-induced epidermal hyperplasia and tumor formation. *Am J Pathol* **162** (6), 2029–2039 (2003).
41. Williams, T. M. *et al.* Loss of caveolin-1 gene expression accelerates the development of dysplastic mammary lesions in tumor-prone transgenic mice. *Mol Biol Cell* **14** (3), 1027–1042 (2003).
42. Volonte, D. & Galbiati, F. Polymerase I and transcript release factor (PTRF)/cavin-1 is a novel regulator of stress-induced premature senescence. *J Biol Chem* **286** (33), 28657–28661 (2011).
43. Kuang, S. Q. *et al.* Aberrant DNA methylation and epigenetic inactivation of Eph receptor tyrosine kinases and ephrin ligands in acute lymphoblastic leukemia. *Blood* **115** (12), 2412–2419 (2010).
44. Winn, R. A. *et al.* Restoration of Wnt-7a expression reverses non-small cell lung cancer cellular transformation through frizzled-9-mediated growth inhibition and promotion of cell differentiation. *J Biol Chem* **280** (20), 19625–19634 (2005).
45. O'Reilly, M. S. *et al.* Endostatin: an endogenous inhibitor of angiogenesis and tumor growth. *Cell* **88** (2), 277–285 (1997).
46. Kaneda, A., Kaminishi, M., Yanagihara, K., Sugimura, T. & Ushijima, T. Identification of silencing of nine genes in human gastric cancers. *Cancer Res* **62** (22), 6645–6650 (2002).
47. Yagi, K. *et al.* Three DNA methylation epigenotypes in human colorectal cancer. *Clin Cancer Res* **16** (1), 21–33 (2010).
48. Suehiro, T. *et al.* Thrombomodulin inhibits intrahepatic spread in human hepatocellular carcinoma. *Hepatology* **21** (5), 1285–1290 (1995).
49. Liu, P. L. *et al.* Decreased expression of thrombomodulin is correlated with tumor cell invasiveness and poor prognosis in nonsmall cell lung cancer. *Mol Carcinog* **49** (10), 874–881 (2010).
50. Marie, H. *et al.* The LIM protein Ajuba is recruited to cadherin-dependent cell junctions through an association with alpha-catenin. *J Biol Chem* **278** (2), 1220–1228 (2003).

51. Hou, Z. *et al.* The LIM protein AJUBA recruits protein arginine methyltransferase 5 to mediate SNAIL-dependent transcriptional repression. *Mol Cell Biol* **28** (10), 3198–3207 (2008).
52. Kanungo, J., Pratt, S. J., Marie, H. & Longmore, G. D. Ajuba, a cytosolic LIM protein, shuttles into the nucleus and affects embryonal cell proliferation and fate decisions. *Mol Biol Cell* **11** (10), 3299–3313 (2000).
53. Carney, D. N. *et al.* Establishment and identification of small cell lung cancer cell lines having classic and variant features. *Cancer Res* **45** (6), 2913–2923 (1985).
54. Sriuranpong, V. *et al.* Notch signaling induces rapid degradation of achaete-scute homolog 1. *Mol Cell Biol* **22** (9), 3129–3139 (2002).
55. Jiang, T. *et al.* Achaete-scute complex homologue 1 regulates tumor-initiating capacity in human small cell lung cancer. *Cancer Res* **69** (3), 845–854 (2009).
56. Kaneda, A. *et al.* Activation of Bmp2-Smad1 signal and its regulation by coordinated alteration of H3K27 trimethylation in Ras-induced senescence. *PLoS Genet* **7** (11), e1002359 (2011).
57. Zhang, Y. *et al.* Model-based analysis of ChIP-Seq (MACS). *Genome Biol* **9** (9), R137 (2008).

Acknowledgements

We thank Kaori Shiina, Hiroko Meguro and Kyoko Fujinaka for their technical assistance. This work was supported in part by Grants-in-Aid for Scientific Research from the Ministry of Education, Culture, Sports, Science and Technology of Japan, the NFAT project from the New Energy and Industrial Technology Development Organization (NEDO), by JST Core Research for Evolutional Science and Technology (CREST) program, and by the Intramural Research Program of the NIH, National Cancer Institute, Center for Cancer Research.

Author contributions

T.S. performed experiments, generated data and figures and co-wrote the manuscript. A.K. designed study, supervised the study, performed experiments, generated data and figures and co-wrote the manuscript. S.T. analysed data and generated figures. T.I. performed experiments. S.Y. analysed data. T.F. analysed data. R.Y. analysed data. Y.T. performed experiments. T.N. supervised the study. V.E.M. performed experiments. Y.I. collected clinical samples and information. M.I. supervised data. H.A. designed study and supervised the study.

Additional information

Supplementary information accompanies this paper at http://www.nature.com/scientificreports

Competing financial interests: The authors declare no competing financial interests.

How to cite this article: Sato, T. *et al.* PRC2 overexpression and PRC2-target gene repression relating to poorer prognosis in small cell lung cancer. *Sci. Rep.* 3, 1911; DOI:10.1038/srep01911 (2013).